Aalto-yliopisto
Aalto-universitetet
Aalto University

Master's Programme in Mechanical Engineering

Characterization of Flexible Support Systems of Large Outfitting Components on Cruise Ships

Aaron Körkkö

Master's Thesis
2022

Abstract

Modern cruise ships are required to have more specialized features and the design process to create them is also more specialized. The isolation of high-end entertainment deck amenities such as basketball courts and glass domes are not intuitive, and the survival of such features demands better characterization of the isolation structural members. Flexible mounting solutions are a viable option and are often characterized with equivalent dynamic stiffness properties to determine how well they survive. This thesis aims to determine the dynamic stiffness properties of two provided flexible mounting devices, one medium sized and one larger sized, by imparting marine-equivalent loads to them and developing the analysis methods to generate characterization information that can be used in further study or in the design of future marine systems.

The data was gathered using a load frame and load cell capable of producing the required frequency and amplitudes of oscillation while preloading the flexible mounting hardware per the marine environment. Preloads of 22.5 kN in compression to 15 kN in tension were performed with simultaneous $1.0 - 20.0$ Hz oscillation frequencies at 0.02mm amplitude. This allows for a preview as to how the mounts would perform in a marine environment. The data is prepared for analysis through parsing, noise removal, high pass filtration, and removal of non-data entries before calculating the equivalent dynamic stiffness using the peak-to-peak slope of the recorded mount force and deflection.

A calibration study is performed, and the data collection method is optimized for each of the testing events. The equivalent dynamic stiffness is reported with values ranging from $15.316 - 41.107$ kN/mm for the larger sized mount, and $5.645 - 11.170$ kN/mm for the medium sized mount.

The two mounts appear to be made of different rubber materials due to the large differences in stiffness between the values calculated, and the larger mount likely approached an asymptotic limit in compression prior to the manufacturer's stated maximum range. The effect of amplitude is briefly reviewed, and tensile loads appear to be more susceptible than compressive loads with respect to equivalent stiffness values. The characterization of the mounts yielded significant results, but also raised more questions as to the phenomena behind them.

Keywords Flexible Mount, Marine Vibration, Equivalent Stiffness, Cruise Ship, Outfitting Components

Contents

Preface

1 Introduction to flexible support systems

1.1 Background

Modern cruise ships are required to have larger and more specialized features than in the past because passengers routinely book tickets based on the reputation of the cruise line, the features available onboard, and the price of the ticket. According to the results of the study by Hie et.al., potential cruisers generally attach more importance to "Recreation and Sport Attributes," "Fitness and Health Attributes," and "Supplementary Attributes" than cruisers during the decision-making process [1]. With this information, cruise ship owners routinely desire to have the largest or newest features which require specialized attention.

Specialized features require more work to accommodate the vibrations caused by feature-created noise such as a basketball court or wave rider or roller coaster. One area of interest is the isolation of the feature from ship-generated noise and vibrations such as engine piston movements and hogging and sagging movements so that they may survive such as intricate glass domes that span several decks. In Figure 1 below, an optional entertainment amenity is shown in the wave rider, which involves several high-volume water pumps to create the wetted surface that allows passengers to surf during their voyage. These pumps and the flowing water introduce new vibration modes which must be accounted for and in many cases isolated so that the passengers who are not utilizing them are undisturbed.

Figure 1: Wave rider passenger amenity [2]

Another feature that is increasingly more common on cruise ships is a basketball court which allows the patrons to remain physically active during the voyage. Figure 2 depicts such a court, and with this feature, the bouncing of a basketball introduces loud noises that transmit through all types of structures and needs to be isolated. Identification of which frequencies are generated is mandatory for successful isolation of the noise. A successful analysis and mitigation plan allows for passenger cabins to be located closer to the amenity and maximizes the intake of passengers and revenue.

Figure 2: Top deck amenity - basketball and sport court [3]

Decorative amenities such as the glass dome in Figure 3 increase the perceived value of the cruise experience to potential customers. These are highly visible and well-advertised to draw in new customers and they serve to improve the experience by creating something beautiful or unique that differentiates one ship from another. The glass dome shown here spans several decks and to properly isolate the load cases from the feature is not obvious, but with careful placement of supports that can flex and prevent a dangerous transmission of loads, they will survive and allow for larger and more ornate domes to be made in the future.

Figure 3: Decorative amenity - glass dome [4]

For all the features mentioned above, proper isolation of these special features requires higher quality mounting devices. This context leads to the interest in flexible mounting devices that can bear weight and accommodate vibrations without translating beyond the coupling point.

1.2 Scope of work

It is desired to isolate amenity features from the hull of the ship due to marine vibrations and the related loading conditions. The crew and passenger cabins onboard any manned ship should be isolated from large outfitting components on the entertainment decks of cruise ships, and from any propulsion and exhausting system vibrations. The process to eliminate the harmful effects of vibrations large and small is not well defined and must be customized for each ship and mission. The exact loading conditions of marine vessels are random and not predictable; but the frequency spectrum of occurrence can be anticipated so long as the operating mission and structural characteristics are understood. Some effects of hull vibrations such as appendage vortices and propulsion noise can be tuned out during sea trials through modification of passive components.

The isolation of noise from the hull is often accomplished using flexible mounting systems which are typically comprised of rubber and metal parts. The composition of two materials must be selected carefully to avoid conditions where they could fail and cause harm to the ship structure or patrons onboard any amenity feature. Rubbers have excellent damping properties and are well-suited to isolate the main ship structure from higher frequency and low amplitude noise generated from small hull deformations. As the hull of the ship deforms due to seaway loading of hogging and sagging, there is a risk of breaking of supports if they are not designed correctly because these types of forces induce large deflections (in the 10s of centimeters). Figure 4 below depicts the main forces due to these loading conditions and every ship that encounters waves will be subjected to the phenomenon.
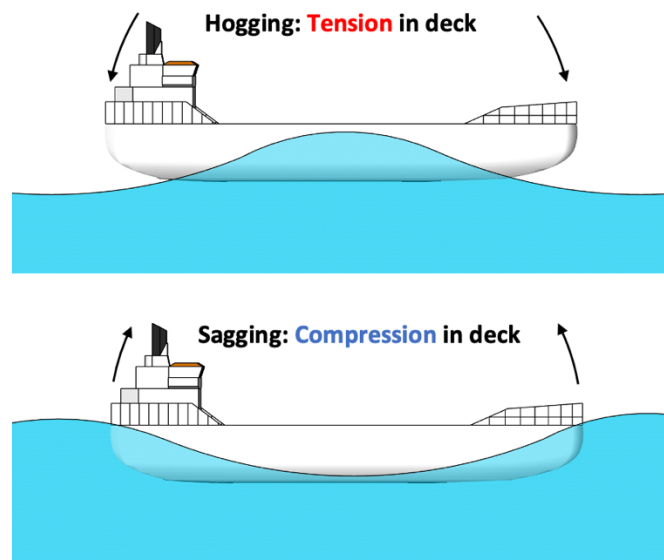
Figure 4: Wave-induced loading diagram

Hogging is the scenario where the crest of a wave is in the center of the hull and tension is experienced on the deck, and sagging is the scenario where the trough of the wave is in the center of the wave and compression is experienced on the deck. These loads have relatively long periods and amplitudes compared to engine noise or other amenity related vibrations and have the potential to cause damage if not accounted for properly.

One solution to avoid damage from large deflections would be to completely disconnect the outfitting component from the hull, and this would be effective- except that local resonances still exist and need to be mitigated. The better approach is to define a frequency spectrum with the anticipated loading and use this to determine the appropriate stiffness required over each vibration frequency and amplitude. This allows the designer to define the margin of performance for the marine mission and can be tested in a laboratory or computer simulation.

The ship vibrations are similar to heavy machinery and earth-moving equipment cases, except that the modes of vibration and forces are more varied for marine environments, so the structures need to accommodate a larger range of frequencies and amplitudes [5] [6]. Factors that are important to these connection points are lightweight design, proximity to propellor, propulsion power, propellor design features, and speed of main engines and depending on the proximity of the flexible mount to any of these factors may result in a different design [5]. The modern cruise ship needs to have robust solutions for noise and vibration isolation and using linear vibration simulations this is achievable when the mounts are accurately understood. Through a literature review, it was found that there are several studies linking the vibration amplitude, frequency, temperature, and specimen geometry to dynamic stiffness and damping characteristics and this thesis aims to recreate the same plots while focusing on the input of preload condition [7]. Preload is important due to the hogging and sagging loads mentioned earlier which impart large forces on marine structures.

The unit under test is an example of a composite flexible support system due to the dissimilar materials being used jointly to accomplish the task of mitigation vibration transmission through the end points. The behavior of the mount is the focus of the work, keeping in mind that rubbers perform better in in compression than tension regarding survivability. The chosen test cases reflect the predicted behavior, and comparisons against state of the art cases will be utilized during the testing.

1.3 State of the art

The use of flexible mounting devices in marine environments is a growing application, which is driven by the need to isolate specialized features from loads and vibrations onboard cruise ships. These systems consist of composite constructions that are tuned to each application and generally are made of a compliant material such as rubber or foam, and a rigid material such as metal or plastic. The stiffness of these mounts does not exactly represent the framework or damping components as it is a combined effect that produces the unique stiffness and damping characteristics. The approximation of these components is that of a single degree of freedom mass-spring system which is shown below in figure 5.
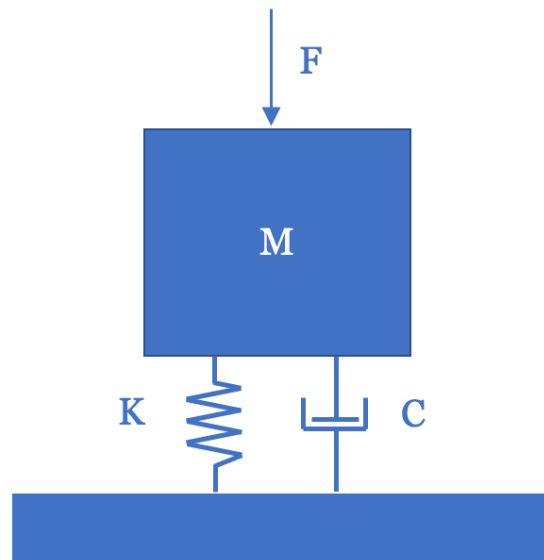

Figure 5: Spring mass damper system [8]

The spring constant- K, damping coefficient- C, and mass- M are the parameters that dictate how the system responds to an impulse of F. For static inputs, the system will behave predictably, but when there is a dynamic load the properties of a system will depend on more complex behaviors such as, frequency of oscillation, damping coefficient, transmissibility, and stiffness. For the mounting systems of interest to this thesis, the stiffness is not constant and is defined as a function of oscillation frequency and amplitude. This can be thought of as a spring that is made of rubber and exhibits behaviors of both springs and rubbers, which are similar but different for energy storage and load transmission. These devices have been used for land- and marine-based structures to absorb unwanted frequencies of piston oscillations in engines, exhaust ducting vibrations, and amenity-generated vibrations.

Rubber is well suited to handle vibrations in many frequencies and depending on the application can handle displacements of up to 10s of centimeters without mechanical failure [9]. The natural properties of rubber have been utilized for many years to dampen harmonic loading; rubber is typically used in passive mounting situations with static and semi-predictable loading conditions. The way rubbers exhibit elastic behavior is due to the strand-like structure within the material which can be stretched or compressed in relation to nearby strands and the movement is inhibited by internal friction forces that help to dissipate the kinetic energy into both potential energy and waste energy in the form of heat [9].

Over time, a rubber mount that is continuously used will become warm from the heat generated and the properties may shift to conditions that are not desirable for the use case [10]. Due to this, special attention is required to utilize a rubber mount to ensure that it will not only perform the required duties at the initial conditions but within the entire operational window. Figure 6 below shows a typical force versus extension for typical rubber materials and for small extensions the curve follows what could be considered a linear model, and then from approximately 50 to 600% extension there is a markedly nonlinear portion before approaching another linear portion with a different modulus than the initial deflection.
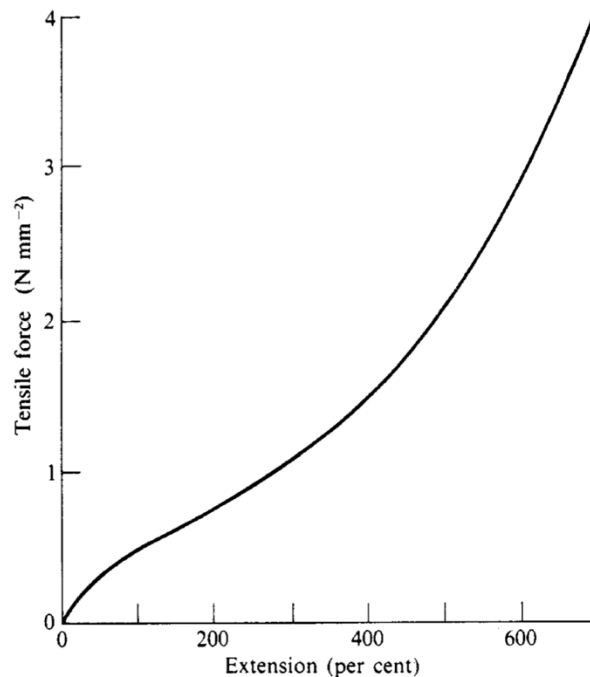

Figure 6: Force v. extension for typical rubbers [7]

This behavior is due to the cross-linking of the rubber strands and as they deflect and strain across each other; the energy is dissipated evenly until the strands begin to stretch beyond the normal limit and cause an extension with relatively small increase in tensile force. With an understanding of the forces and conditions imparted onto the rubber pieces, rough estimates can be made regarding the lifecycle of the components, but in-situ testing and verification will increase the understanding of the use case for future applications. The typical force-extension curve for rubber materials is non-linear by nature and only in small strains (<10%) can the modulus be approximated as linear [7] [11].

Rubber can be molded into many shapes with ease, but not all geometries provide adequate damping in all situations so thorough understanding of the capabilities and strengths and weaknesses is required to properly utilize this material in real world scenarios. Additives are often combined with rubbers to make them more chemically resistant, to modify the conductivity, boost hardness values, or increase temperature resistance [7] [11] [9] [12]. Once the additives and fillers are added the best way to predict how it will perform is to utilize design tables that show what effect adding certain particles or chemicals has. If the additive is not widely understood or does not have empirical data, test specimens should be created and tested to verify the stress/strain curves, ultimate strength, and other metrics of the material. Tables exist with many types of rubbers and compliant materials, but another factor in the design process is the use case- whether it will be used in tension or compression, the environmental conditions of temperature and exposure to UV, and the frequency of loading and unloading are all important features to consider.

Flexible mounting solutions for land-based environments are used to mitigate seismic shifts in buildings, isolate vibrations from railway or other heavy traffic vehicles, as sound isolation in buildings that have multi-use spaces, and in construction vehicle mounts [13] [6] [14]. One land-based solution is with regards to concrete barriers that are meant to withstand impact- a study carried out by Rahman et al it was shown that when adding up to 10% scrap rubber from used tires into concrete beams, the anti-vibration properties of such beams compared to an all-concrete version were increased and the natural frequencies were also reduced.

Figure 7 below shows the test setup for a concrete beam which was researched to improve properties as an effective barrier for vehicle or other moving object impacts.

Figure 7: Bend test setup for rubber-filled concrete [15]

While this concrete material is not feasible to use in marine environments due to excessive mass, the methods and attention to details are noteworthy and beneficial to realize. The outcome of the study demonstrates that for certain applications there could be a solution that requires no modification to the mounting style or dimensions and could be only a composition change, such as adding waste rubber into the raw material.

Another land-based solution is engine mounts made of rubber, which have been used for over 100 years and effectively isolate the running engine vibrations. The shape of the rubber and metal connections are important as well as the characteristics of the engine and weight distribution, but effective isolation through smart mounting design is possible as seen in the Harley Davidson dissertation in 2013. The rubber mounts in this application are passive in nature and must be tuned to accept all possible frequencies and amplitudes of vibration. Figure 8 below shows the mounting locations of a motorcycle engine, each of which is required to have damping properties to improve the experience of the rider to prevent fatigue injuries and extend the life of the welded joints on the vehicle.
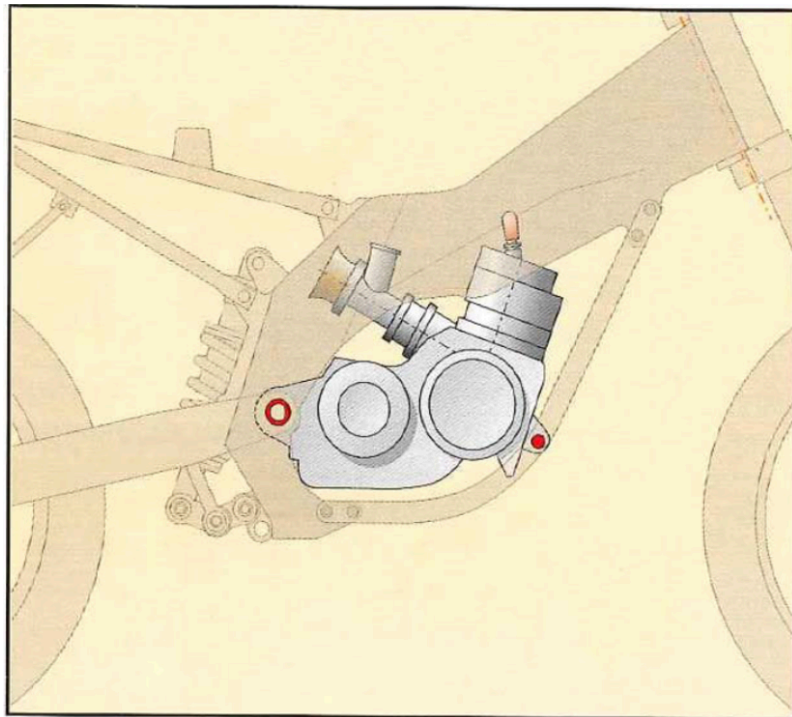

Figure 8: Motorcycle engine mount 12 DOF model [14]

These studies are significant because they demonstrate that with proper understanding of the loading conditions and characterization of the compliant materials, important advances in the design of a system can be achieved. Marine- and land-based applications for vibration isolation are similar, but have different conditions that must be considered, which necessitates an experimental investigation to find the stiffness properties of the flexible mounting elements.

To utilize flexible mounts in applications where a significant and variable structural load is carried through them requires characterization of the dynamic stiffness behavior. When a rubber unfilled specimen is subjected to cyclic loading in a harmonic manner, the hysteresis loop can be approximated as follows in a linear slope which is shown below in Figure 9.
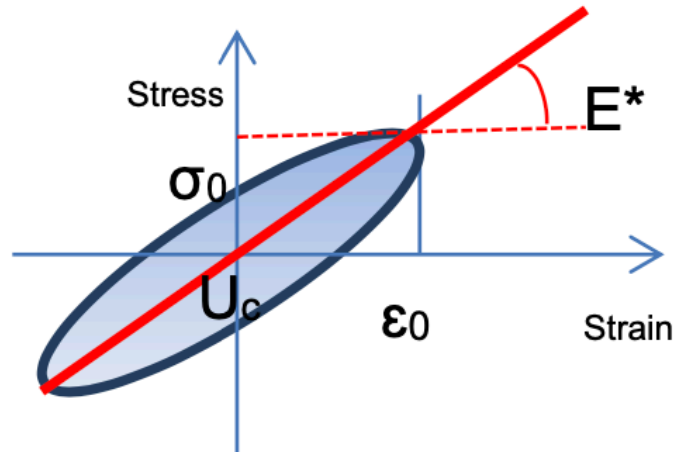

Figure 9: Linear viscoelastic hysteresis loop for harmonic excitation [7]

The initial loading case is shown as U_C in [kN], stress and strain is given as σ_0 and ε_0 in [kN] and [mm] respectively, and the equivalent modulus E^* is known as the storage modulus with units of [kN/mm], which represents the real portion of the complex modulus used to describe rubber behavior [7]. This nonlinear elliptical loop is associated with the dissipated energy of the rubber U_C and is related to the storage of elastic energy, subsequent dissipation of potential energy, and the breakdown and reforming of the rubber structure. For the purposes of the thesis, the closest approximation of the mount is that of a rubber spring, which follows this behavior and will be used to generate the storage modulus for the purposes of comparison.

Figure 10 below shows the effect of a static preload combined with a dynamically applied load to the specimen. The initial modulus captured by static testing is calculated by utilizing σ_p and ε_p and is markedly different than the storage modulus of E^* which uses σ_0 and ε_0 as the parameters.
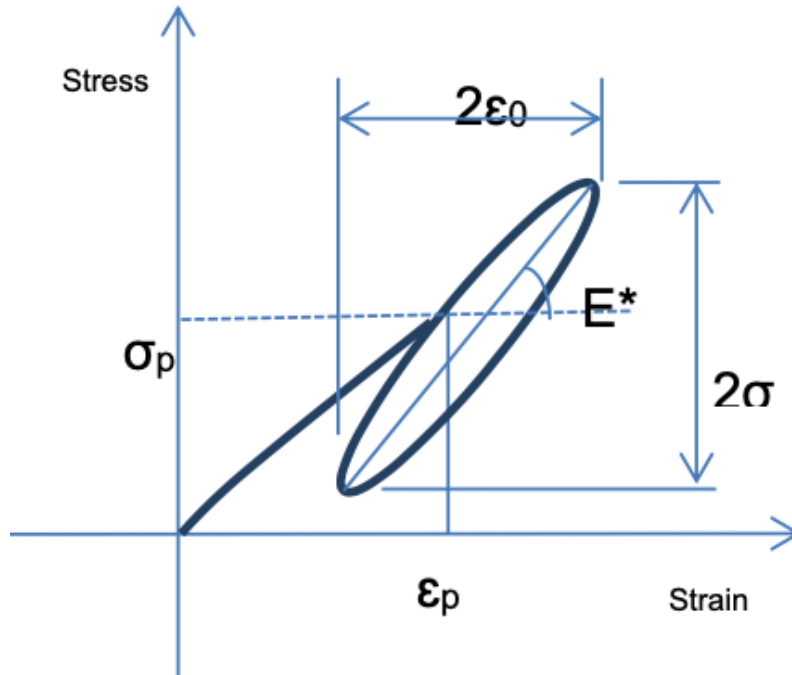

Figure 10: Static preload and dynamically applied load [7]

For rubber materials that have drastically changing loading conditions, the storage modulus and that of the initial deflection must be considered during the lifetime of the components.

With higher amplitudes the dynamic modulus decreases due to higher breakdown rates, and the dependence of stiffness is related to a stress-softening phenomenon known as the "Mullins effect" [7]. When the amplitudes of oscillation are small, there is only a small structure which is broken down and the storage modulus mentioned above is not modified. For the purposes of this thesis work, the oscillation amplitudes are considered small, and only minimal Mullin's effect is expected.

1.4 Thesis objectives

The focus of the thesis is to study the dynamic stiffness of a flexible mounting apparatus and to contribute to the understanding of the properties of these devices. With better understanding of the important factors, designs within passenger ship structures and the influence of preload and frequency on dynamic stiffness can be obtained. The chosen amplitude and frequency parameters are taken from a cruise ship application and fall within the manufacturer's recommended usage window. The dynamic stiffness is calculated using two different size mounts to enable comparative analysis to be performed. The intention of this thesis is to generate stiffness parameters so that a linear vibration analysis can be performed with confidence, as previous simulations created solutions that were not sensible and further fidelity was desired.

The information collected in this thesis will provide understanding to the previously unknown characteristics of flexible mounting systems used in load-bearing applications. The results and methods utilized will be used in the future to determine whether stiffness values can be properly modeled in a finite element simulation to assist with cruise ship design. The demand exists to uncover the relationships between preloads, vibration frequencies, and vibration amplitudes for flexible mounting components. The experimental study aims to relate the terms of preload, stress, and strain to characterize the mount and create a base understanding from which additional study is possible.

Several research questions are posed in the characterization effort in this thesis including the following: What technologies exist as solutions to flexible structures in ship- and land-based constructions? How do we develop the test methods for different elements of the assembly structures? What happens to the system when there is a combined effect? i.e., large deflection with constant vibration or small deflection with changing vibration? Are the properties of a system able to be scaled up or down effectively?
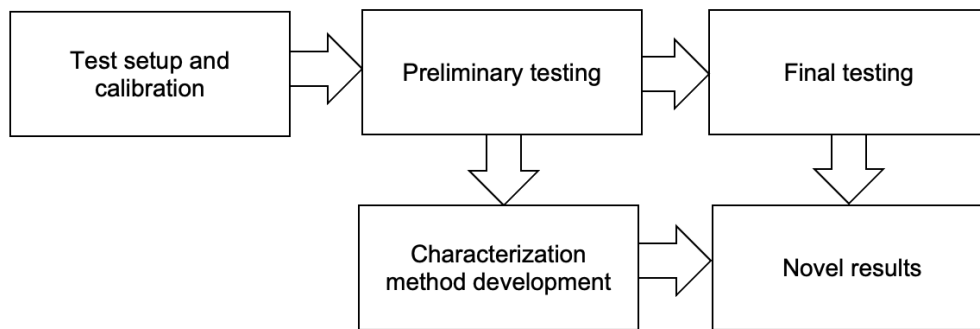
1.5 Limitations

This thesis is limited in scope to review the equivalent stiffness characteristics of flexible mounting devices and not the damping properties. The primary interest area is the dynamic stiffness with respect to preloaded value and the frequency of vibration as this is relevant to the use case of the cruise ship marine environment. The data collection method utilized in the case study is simplified and may not represent a true loading scenario, but the test setup allowed for meaningful data to be collected with the resources that were available during the evaluation period. The detailed characterization of flexible mounting devices requires much more testing than was performed in this thesis, but the results provided interaction data that allows for further testing in different configurations.

For practical data collection in this thesis, only one type of composite flexible mounting device is tested. This is provided by Meyer Turku and is a possible mount for implementation in future designs in cruise ship environments. The mount is chosen due to the high tensile and compressive loads that it is rated for and the oscillation frequency properties. The information available on how it performs with changing loading patterns and oscillation frequencies was unknown and worthy of further study and is the primary reason why it was chosen to undergo testing.

The organization of the thesis is as follows; methodology is presented first with discussion of the approach to understanding the subject with a focus on equivalent stiffness, the results from the data collection follows with interpretation of the graphs and data ranges as necessary, the discussion section is next with the behavior of the mounting device compared against state of the art and other notable trends and comments regarding sources of error and credibility of results, and the conclusions is last with final thoughts regarding the most significant contributions to the characterization of the mounts and answers to the research questions posed in the introduction. The text concludes with further questions raised during this study, a list of references, list of figures, and an appendix with MATLAB code and some mechanical drawings to recreate the mechanical adapters.

2 Methodology

In this section the information pertaining to the testing hardware, data handling and analysis, and approach for calculating the dynamic stiffness are detailed. The test articles, required adapters, and support equipment are introduced, and the important details are discussed with the proposed loading parameters for a calibration study, and more formalized stiffness study. Following the test setup, the methods of data analysis are introduced including removal of non-numbers from the raw data, filtering of the signal to reduce noise, and the removal of end effects due to the test cell oscillation ramping behavior. In the last section, the analysis of the data is proposed for calculating the equivalent dynamic stiffness using the hysteresis loop and local maxima and minima to generate the required characterization details. The overall methodology process is described in the flowchart below. The test setup and calibration step is the first task, which results in preliminary testing and the development for the method to characterize the mount, which leads to final testing and analysis and novel results.

```
┌──────────────────┐      ┌──────────────────┐      ┌──────────────────┐
│  Test setup and  │ ═══▷ │ Preliminary      │ ═══▷ │  Final testing   │
│   calibration    │      │     testing      │      │                  │
└──────────────────┘      └──────────────────┘      └──────────────────┘
                                    ║                          ║
                                    ▽                          ▽
                          ┌──────────────────┐      ┌──────────────────┐
                          │ Characterization │ ═══▷ │   Novel results  │
                          │ method development│      │                  │
                          └──────────────────┘      └──────────────────┘
```

2.1 Test setup

The Broneske M01 and L01 mounts are described in Table 1 below; they are the primary source of characterization for this thesis. The test articles used in this case study are provided by Meyer Turku and consist of two SB Broneske Anchorage Points: Tension-Compression Mount SBB61001-10002 and Tension-Compression Mount SBB61003-10002. The former is identified as M01 for "medium" mount size and serial number 01, and the latter is identified as L01 for "large" mount size and serial number 01.

Table 1: Units under test for thesis [16]

Mount	Serial Number	Load Low [kN]	Load High [kN]	Weight [kg]
M01	SB61002-00002	3.000	10.00	5.8
L01	SB61003-00002	10.00	30.00	10.0

Table 2 below describes all the equipment used for data collection in the case studies. The test setup consists of the MTS 810 Material Test System, custom mounting adapters, and test articles M01 and L01 and pneumatic clamps 647 Hydraulic Wedge Grips, which will be presented in the figures that follow.

Table 2: Equipment list

Article	Manufacturer	Model
Load frame	MTS	810 Material Test System
Load cell	MTS	609 Alignment Fixture 100 kN
Test computer	MTS	Windows XP Data Center
Test apparatus	MTS	647 Hydraulic Wedge Grip
M01 mount	SB Broneske	SBB61003-10002
L01 mount	SB Broneske	SBB61002-10002
M20 adapter LH	Aalto University	M20_mount_left
M20 adapter RH	Aalto University	M20_mount_right
M24 adapter LH	Aalto University	M24_mount_left
M24 adapter RH	Aalto University	M24_mount_right

After the flexible mounting devices and test system were decided, the next task to create custom adapters to interface between the load cell, flexible mounts, and load frame hydraulic cylinder. Several designs were evaluated, and the following was chosen due to its simplicity and robustness. The adapters are machined from mild steel to attach to the threaded ends of the mounting devices and to allow the hydraulic clamps of the MTS testing system to properly interface with the ends. The interface area between the clamps and adapter was maximized to prevent any slipping that could occur and allow for the best transfer of power from the hydraulic system to the mounting device itself. A minimum of 5 threads of engagement was the design criteria to ensure the mechanical connection was adequate under load.

Figure 11 below shows the geometry of the custom adapters which were created at Aalto University's mechanical fabrication center. The mechanical drawings generated to fabricate these adapters can be found in appendix section 8.1 and contain the pertinent dimensions that interface with the MTS clamping system and the Broneske M01 and L01 mounts.
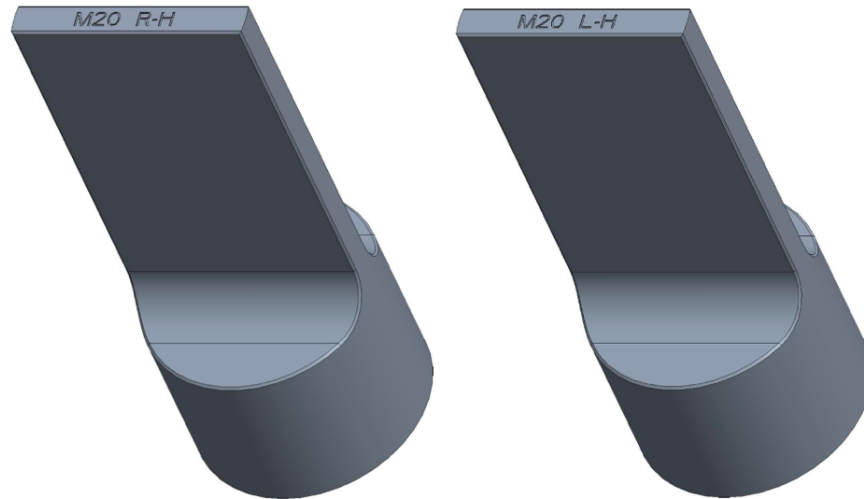

Figure 11: M20 mounting adapters, manufactured from mild steel

After the adapters were manufactured, the test fitting onto the hardware showed no issues and there was proper engagement with threading and the hydraulic clamps on the load frame. Figure 12 below shows the mounting device with the mild steel adapters installed, which allows for the translation of load to the middle section of the flexible mounts M01 and L01.
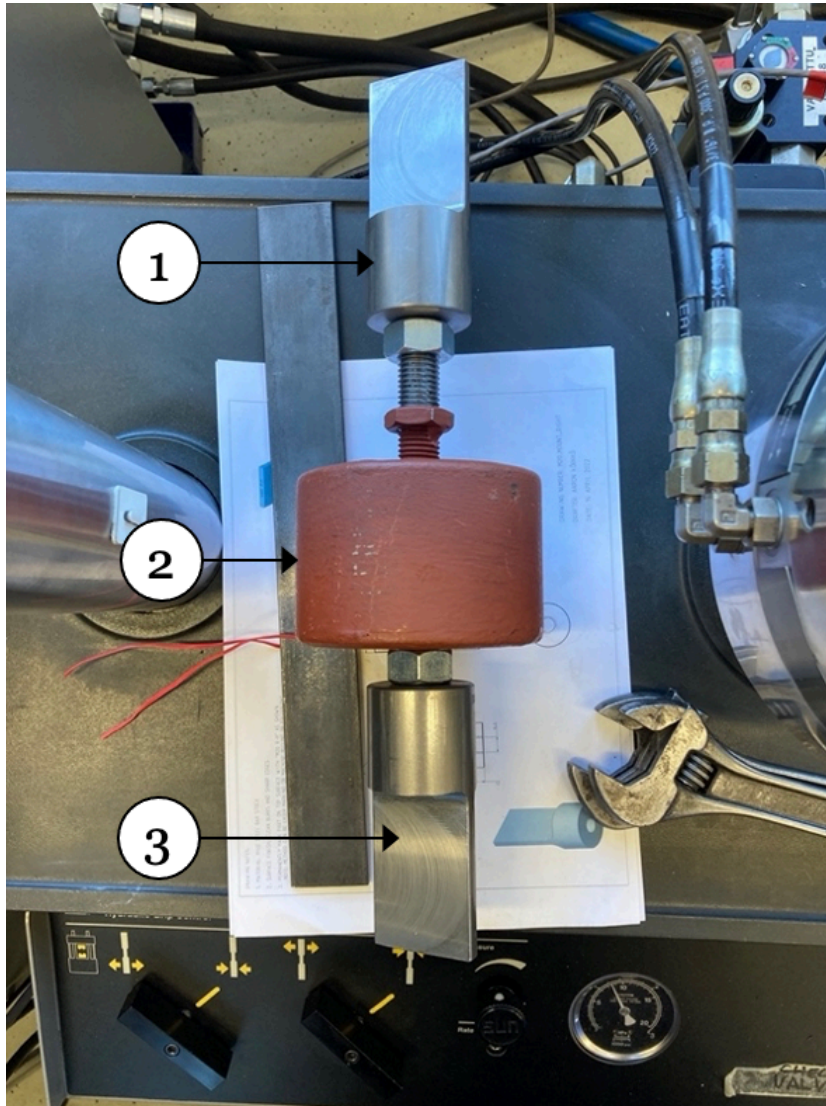
Figure 12: Mounting device, 1: M20 LH adapter, 2: M01 mount, 3: M20 RH adapter

The test system prior to mount installation is shown in Figure 13 and is in the Aalto University Solid Mechanics Laboratory. The load frame is capable of precise measuring and recording of force and displacement for the required tests and is equipped to handle oscillation testing of the same variety that needs to be performed.
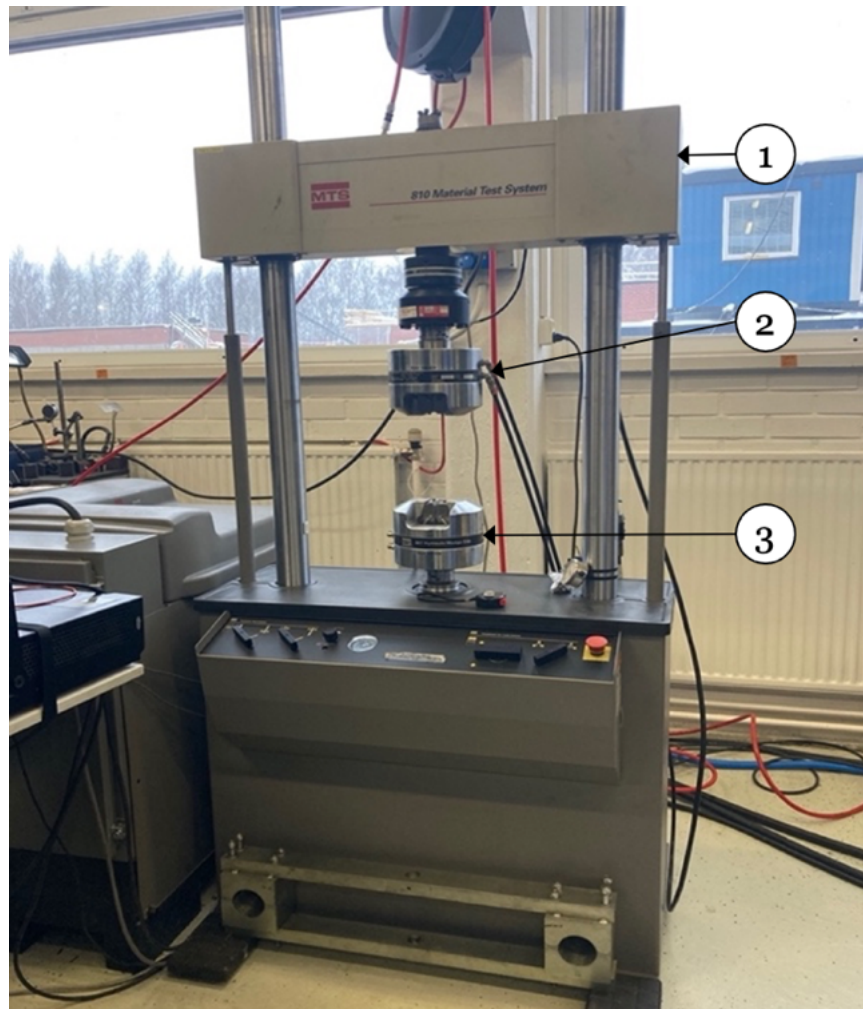
Figure 13: Test System- 1: Load frame, 2: Load cell, 3: Test apparatus

There exists another testing system in the Solid Mechanics Laboratory with a temperature-controlled chamber and larger force capability, but it was deemed unnecessary at this stage of the characterization, and the room conditioned system performed all the necessary tasks to generate the initial characterization profiles.

The data sampling rate of the test system is maximized at 1048 Hz. The tester is controlled by a Windows XP machine with the interface shown below in Figure 14. Real-time monitoring of amplitude, frequency, and preload was necessary to complete this testing and this terminal accomplished the task.
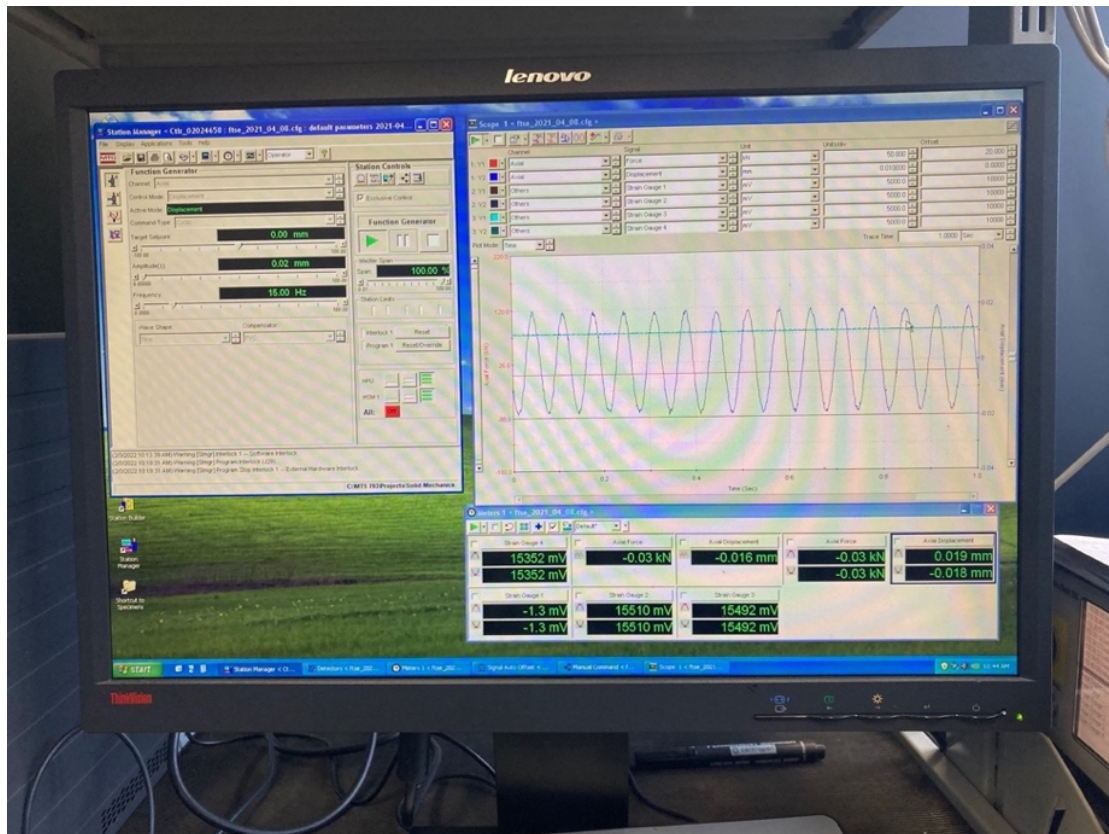

Figure 14: Test cell workstation

The data collection was performed locally and transferred to a local hard drive via USB stick for data preparation and analysis. It was found during the initial study that the maximum sampling rate was sufficient for frequencies up to 20 Hz but beyond that range, there was degradation of force impulse characteristics, and the limit of 20 Hz was imposed for the detailed characterization study.

The loading cell is shown in Figure 15 below and is capable of 100 kN loading. This is used to record the force values which range from 22.5 kN in compression to 15 kN in tension for the larger mount L01 and from 9.5 kN in compression to 4.5 kN in tension for the medium sized mount M01. There were no concerns regarding fixture integrity for the duration of testing and after all testing was completed there were no signs of plastic deformation on any component used during the test.
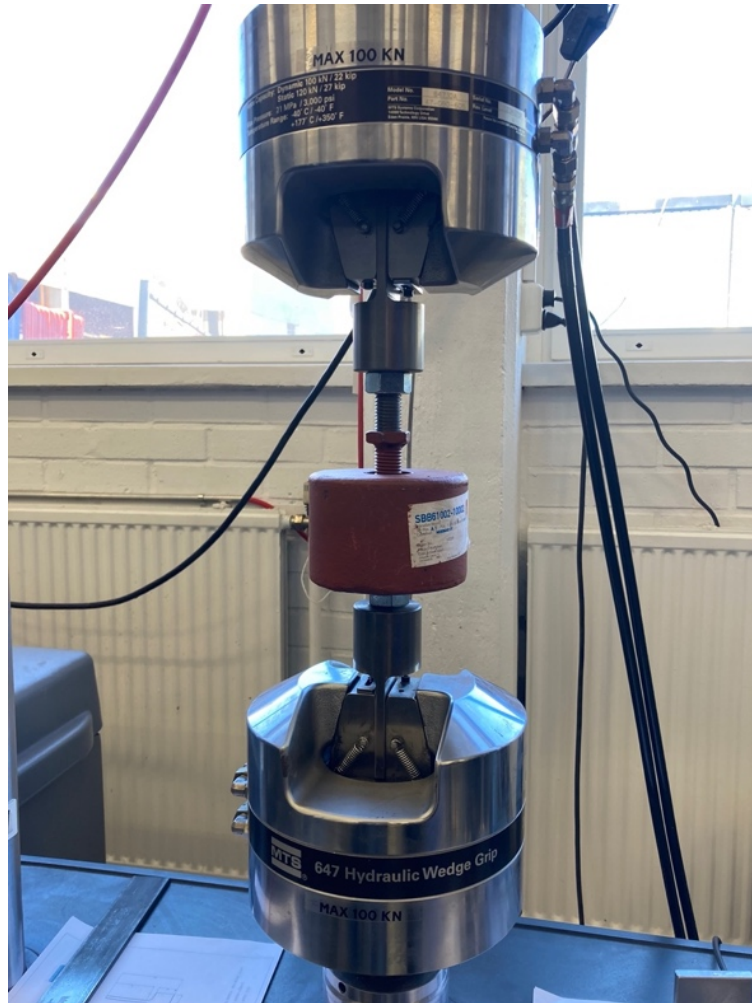

Figure 15: M01 mount installed into load frame

The tables below show what the loading parameters are for the planned tests in this thesis. The initial calibration study is shown in Table 3, and was used to develop the data collection method and analysis, and Table 4 and Table 5 represent the comprehensive review of the desired frequencies of oscillation. The testing was performed in the Aalto University Solid Mechanics Laboratory on 13 May 2022, 16 May 2022, and 27 July 2022 at room conditions and the data analysis occurred in the following months.

Table 3: Calibration study - loading parameters for M01

Preload [kN]	Amplitude [mm]	Frequencies [Hz]
4.50	0.020	5.0, 10.0, 20.0, 25.0
2.50	0.020	5.0, 10.0, 20.0, 25.0
0.00	0.020	5.0, 10.0, 20.0, 25.0
-5.00	0.020	5.0, 10.0, 20.0, 25.0
-2.50	0.020	5.0, 10.0, 20.0, 25.0
-7.50	0.020	5.0, 10.0, 20.0, 25.0
-9.50	0.020	5.0, 10.0, 20.0, 25.0

The calibration study was designed to test the sensitivity of the hardware and test equipment to modifications in preload and oscillation frequency. The smaller mount was chosen arbitrarily, and the parameter range of preload and frequency was decided upon to generate enough data in both axes to notice any shifts in mount behavior. Through researching the differences in behavior of rubber mounts in tension and compression, it was determined to test the full manufacturer's range in compression but not the same span in tension due to concerns of damage to the internal fibers of the rubber portion of the mount [7]. The number of test articles was limited so the collection methods were cautious to ensure the most data could be collected before inducing failure modes and the subsequent effect on the equivalent stiffness readings.

In Table 4 and Table 5 below, the loading parameters were optimized for the equivalent stiffness calculations and to further expand the fidelity of the operating window. They were decided based on results from the calibration study and to avoid inadequate sampling rates which were discovered above 25 Hz oscillation. The preload values remained similar on the M01 mount, and for the L01 mount a change in amplitude for two loading cases was added to preview what effect this modification has on the mounting device.

Table 4: Loading parameters for L01 to determine equivalent stiffness

Preload [kN]	Amplitude [mm]	Frequencies [Hz]
0.00	0.020	1.0, 2.5, 5.0, 7.5, 10.0, 12.5, 15.0, 17.5, 20.0
0.00	0.020	1.0, 2.5, 5.0, 7.5, 10.0, 12.5, 15.0, 17.5, 20.0
-7.50	0.020	1.0, 2.5, 5.0, 7.5, 10.0, 12.5, 15.0, 17.5, 20.0
7.50	0.020	1.0, 2.5, 5.0, 7.5, 10.0, 12.5, 15.0, 17.5, 20.0
15.00	0.020	1.0, 2.5, 5.0, 7.5, 10.0, 12.5, 15.0, 17.5, 20.0
-15.00	0.020	1.0, 2.5, 5.0, 7.5, 10.0, 12.5, 15.0, 17.5, 20.0
-22.50	0.020	1.0, 2.5, 5.0, 7.5, 10.0, 12.5, 15.0, 17.5, 20.0
7.50	0.040	1.0, 2.5, 5.0, 7.5, 10.0, 12.5, 15.0, 17.5, 20.0
-7.50	0.040	1.0, 2.5, 5.0, 7.5, 10.0, 12.5, 15.0, 17.5, 20.0

Table 5: Loading parameters for M01 to determine equivalent stiffness

Preload [kN]	Amplitude [mm]	Frequencies [Hz]
5.00	0.020	1.0, 2.5, 5.0, 7.5, 10.0, 12.5, 15.0, 17.5, 20.0
-9.00	0.020	1.0, 2.5, 5.0, 7.5, 10.0, 12.5, 15.0, 17.5, 20.0
-7.50	0.020	1.0, 2.5, 5.0, 7.5, 10.0, 12.5, 15.0, 17.5, 20.0
-5.00	0.020	1.0, 2.5, 5.0, 7.5, 10.0, 12.5, 15.0, 17.5, 20.0
-2.50	0.020	1.0, 2.5, 5.0, 7.5, 10.0, 12.5, 15.0, 17.5, 20.0
0.00	0.020	1.0, 2.5, 5.0, 7.5, 10.0, 12.5, 15.0, 17.5, 20.0
7.50	0.020	1.0, 2.5, 5.0, 7.5, 10.0, 12.5, 15.0, 17.5, 20.0

2.2 Preparation of raw data for analysis

The datafiles for each test case were generated using the MTS software to export the parameters of running time, time, axial force, axial displacement, and axial count. Running time is obtained from the system load frame clock, time is from the data collection software, axial force and displacement is reported by the load cell and is used for analysis, and axial count is a logical value that should only increase and is used for troubleshooting. The information is loaded into MATLAB using a script which delineates the information into separate arrays which are assigned as time, force, displacement, and count. The time variable was chosen to be the "time" instead of "running time" due to the agreement of values but also because all three came from the same recording device.

Table 6 below shows an example of the raw data from the .txt file that is used for all analysis in MATLAB.

Table 6: Case study #1 sample dataset

Running time [sec]	Time [sec]	Axial force [kN]	Axial displacement	Axial count [segments]
93.331055	93.333008	-7.2469511	-2.0841408	3721
93.356445	93.358398	-7.4683304	-2.116261	3722
93.380859	93.382813	-7.2392669	-2.0839593	3723
93.40625	93.408203	-7.4742002	-2.1159732	3724
93.431641	93.433594	-7.2609587	-2.0841315	3725

During the initial analysis, the data was found to have nans (not-a-number) and other incomplete entries, which caused the mathematical operations in MATLAB to fail, so a process to identify and remove these problem entries was developed. This method was not intuitive for removal and the process was as follows; find the indices of nans in the initial time matrix and store them into a 'purge' matrix, then flip the order so that the order of indices is reversed, and the highest entries are first, then run a for loop that reads in the values from this purge matrix and nulls the corresponding data values for all parameters.

The removal of the nans allows for mathematical operations to continue, but it is also required to remove corresponding data from other matrices so that all data points are intact and not matched with new timestamps for example. This process is repeated for the force and displacement matrices in case one matrix has more corrupted entries than others.

After the data was processed to only include real numbers, the data was subjected to a signal filtration step to prevent noise properties from obscuring the cycle counts. Figure 16 below shows the effect of the signal filtering, which was accomplished using a MATLAB filtration function with a window size of 10 data points. The 1-dimensional filter in MATLAB is a rational transfer function which is expressed as a difference equation with the number of terms equal to the n value.
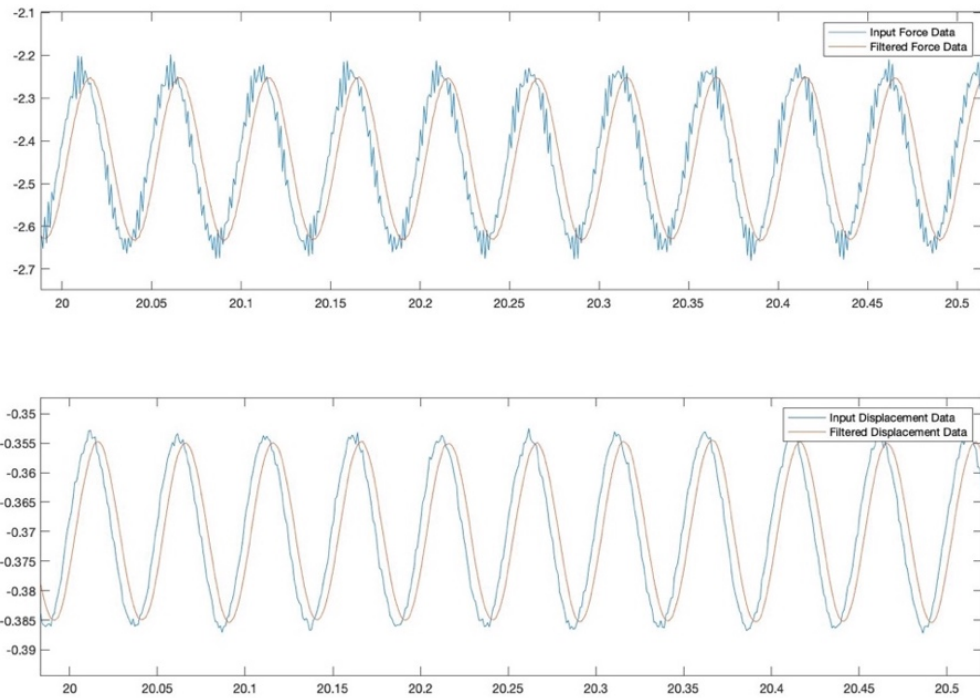

Figure 16: Filtering using MATLAB filter function window size 10

The rational transfer function can be represented by the difference equation as in Equation 1 and the direct form implementation as in Figure 17 below. These representations show that the filtered term depends on the adjacent terms to reduce the sharp transitions that are attributed to noise in the signal [17].

$$
\begin{aligned}
a(1)y(n) = b(1)x(n) + b(2)x(n-1) + \cdots + b(n_b + 1)x(n - n_b) \\
-a(2)y(n-1) - \cdots - a(n_a + 1)y(n - n_a)
\end{aligned}
\tag{1}
$$
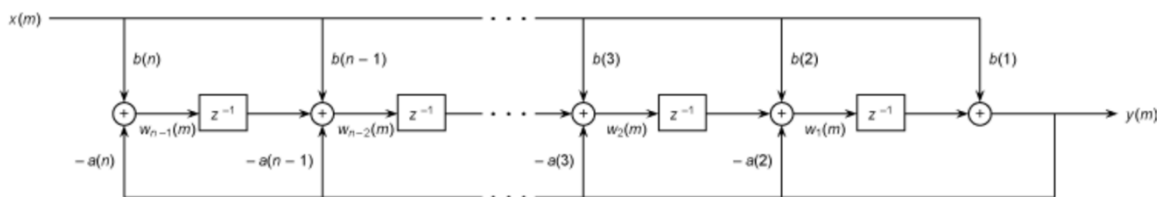
Figure 17: MATLAB rational transfer function diagram [17]

A window size of 10 was found to be adequate for all cases except for 25 Hz where the limitations of the data acquisition caused the post-processed data to be adversely affected by clipping each peak and causing the period to shift from the actual values. Due to the discovery of the filter function not being able to function properly at 25.0 Hz due to insufficient sample frequency, the final list of frequencies to be tested did not include values higher than 20.0 Hz.

After the invalid cells are removed and the data is filtered, the force and displacement variables are plotted against time to determine whether the test provided useful data for analysis. The tests for the first case study began recording while the hydraulic cylinder was static so there are end effects which detract from the data quality. Figure 18 below shows the desired test data area outlined with a dotted line.
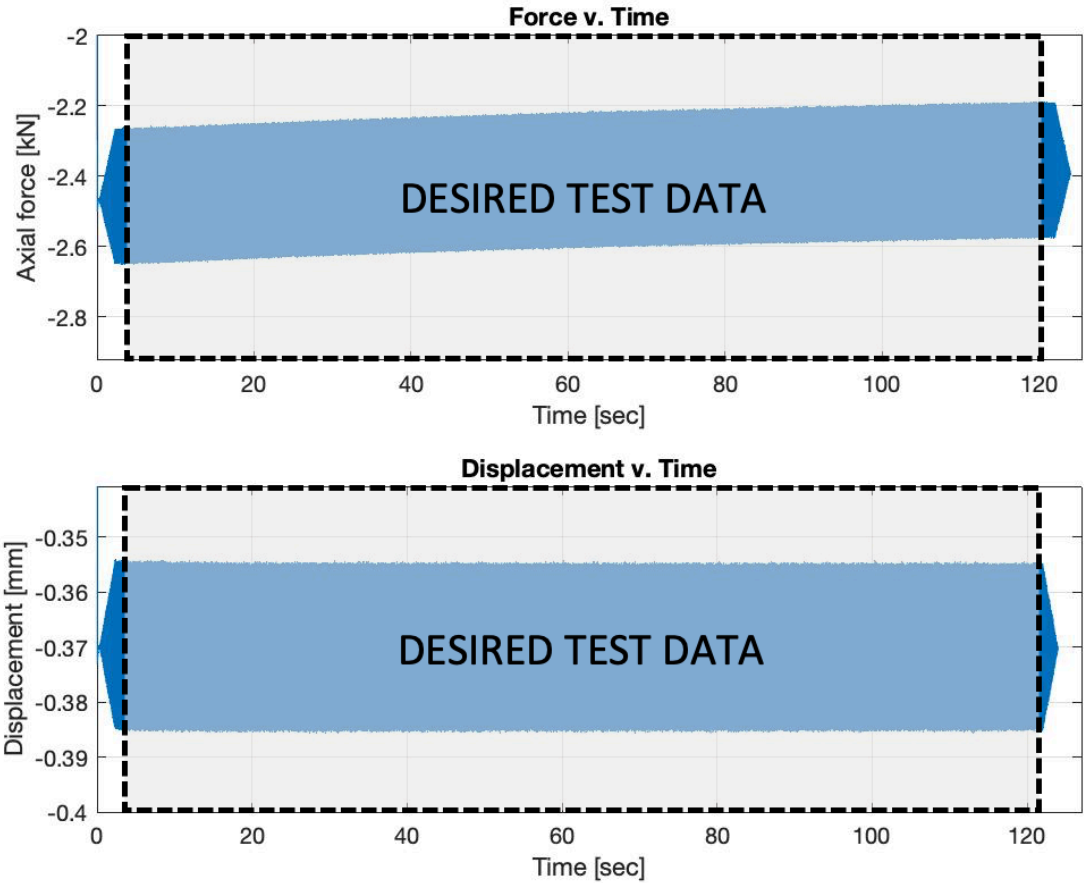
Figure 18: Force and displacement desired test data window

The end effects still provide valuable data but since there was adequate 'good' data available they were ignored for sake of simplicity in these test runs. The end effects were removed manually for the first portion of testing and then the test method was modified to prevent them from occurring in subsequent tests.

For each of the test runs, the start and stop time was manually recorded and transcribed into the MATLAB code for each of the preload and vibration frequency cases. This was performed to prevent these end effects from obscuring the final values of the stiffness at each frequency and preload. The amount of data removed was less than 5% and was not believed to cause aliasing as it only removed transient cycles with changing amplitudes. Figure 19 below shows the dataset that has the end effects removed and is ready for final analysis.
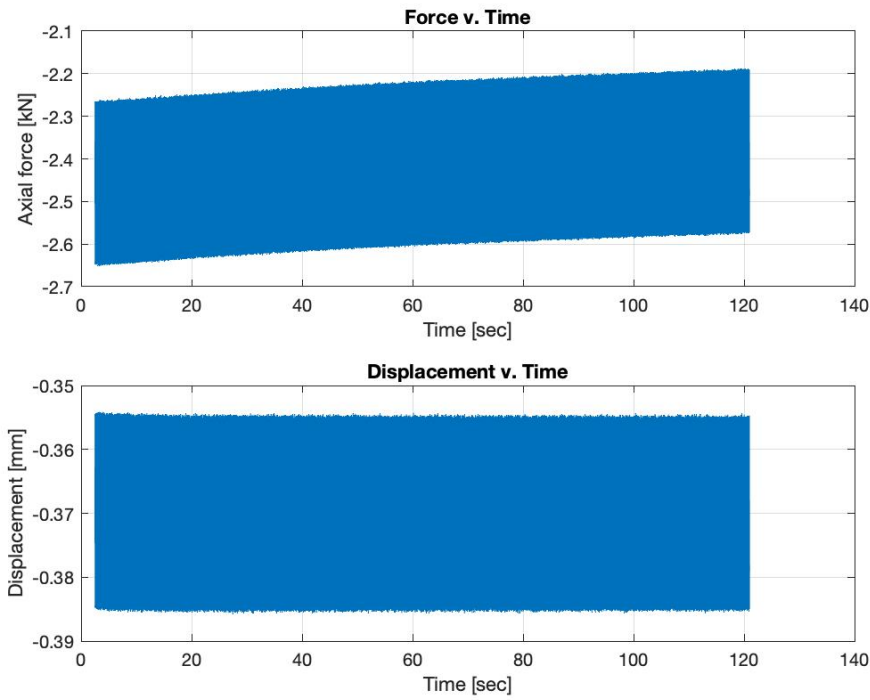
Figure 19: Prepared dataset with end effects removed

The calibration study showed there was excessive drifting in the force measurements which caused the calculation of the dynamic stiffness to be obscured. The solution to the drifting was to impose a high pass filter within MATLAB that sampled the data at a minimum of 100 times the fastest oscillation frequency and filtered out any low frequency signals at half the slowest oscillation or less to prevent any low frequency signal shifting to detract from the results. Figure 20 below shows the effect of the high pass filter on the time history of the force recording for a given test. The orange is the correction of the blue raw data, and it appears to have no drift which allows for the best calculation of the equivalent stiffnesses.
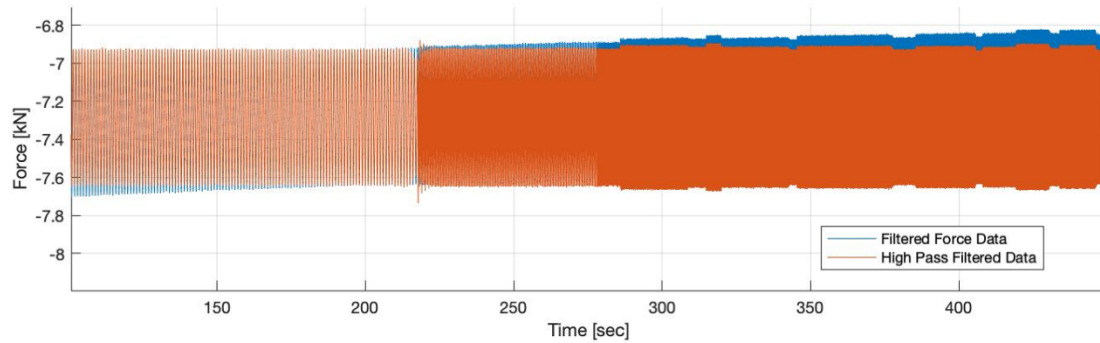
Figure 20: Data with high pass filter effects shown

In the next section, the presentation of the mathematical methods to determine equivalent dynamic stiffness are presented and a brief comment regarding the static stiffness calculation, which was not the primary focus of the thesis and included as a verification tool to determine basic properties of the mounting device.

2.3 Methods used to calculate equivalent dynamic stiffness

The equivalent stiffness is calculated by performing the data preparation methods mentioned in the sections earlier, and then utilizing the maximum and minimum values of the harmonic oscillation hysteresis loop for both force (in kN) and displacement (in mm) to calculate an equivalent stiffness (in kN/mm). Equation 2 below shows the values required to calculate the stiffness at a given preload and frequency of oscillation.

$$k_{equiv} = \frac{F_1 - F_2}{x_1 - x_2} \tag{2}$$

The maximum and minimum values are obtained from the datasets in MATLAB using a maximum and minimum search function for both the force and displacement parameters, and the slope is calculated and recorded for further analysis.

Figure 21 below shows the values of force and displacement plotted against time for visualization of the values in a practical sense, with the force values obtained on the right y-axis being approximately -6.91 kN and -7.65 kN for F_2 and F_1, respectively, and the displacement values obtained on the left y-axis being approximately 0.019 mm and -0.018 mm for x_2 and x_1, respectively. Utilization of equation 2 gives the equivalent stiffness of approximately 20.0 kN/mm.
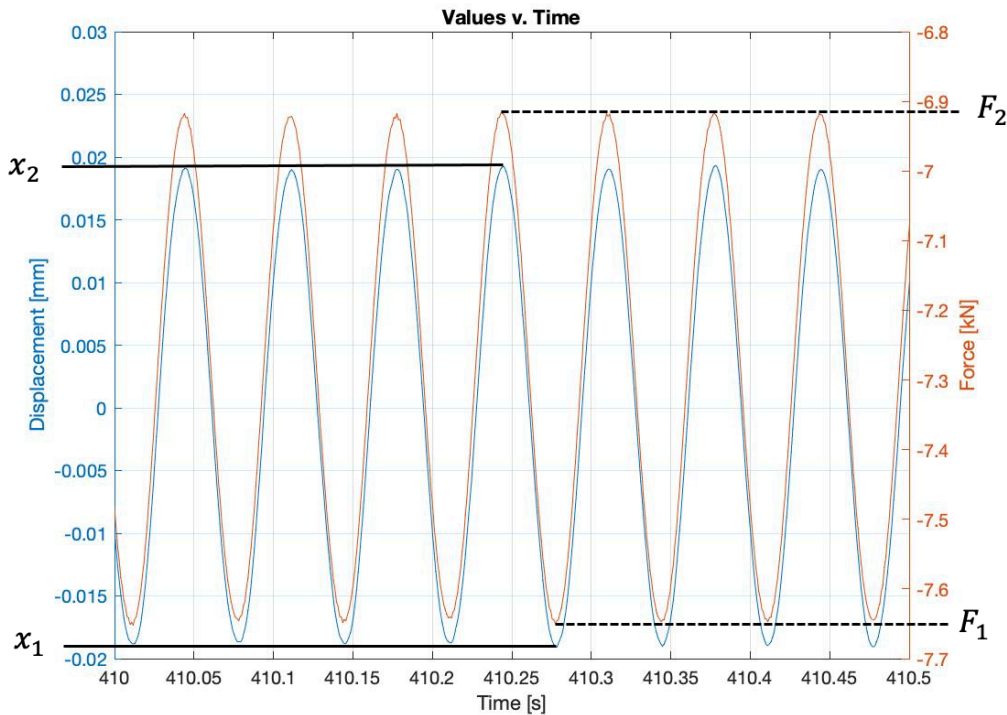
Figure 21: Example time histories of force and displacement

34

It is noteworthy that for this small dataset, the calculated equivalent stiffness value might not match that of the entire set, which is why MATLAB is utilized to find the absolute maximum and minimum during the duration of the test. The value stated above is for reference only to better understand the calculation method.

Figure 22 below represents the full dataset of all the oscillations and is a better approximation for obtaining the equivalent stiffness. The hysteresis loop is bound by the maxima and minima of force and displacement and used for calculating the stiffness that is further analyzed in the discussion and conclusion sections. The largest peak-to-peak value in force and corresponding displacement are used to generate the tables of results and subsequent visualization graphs.
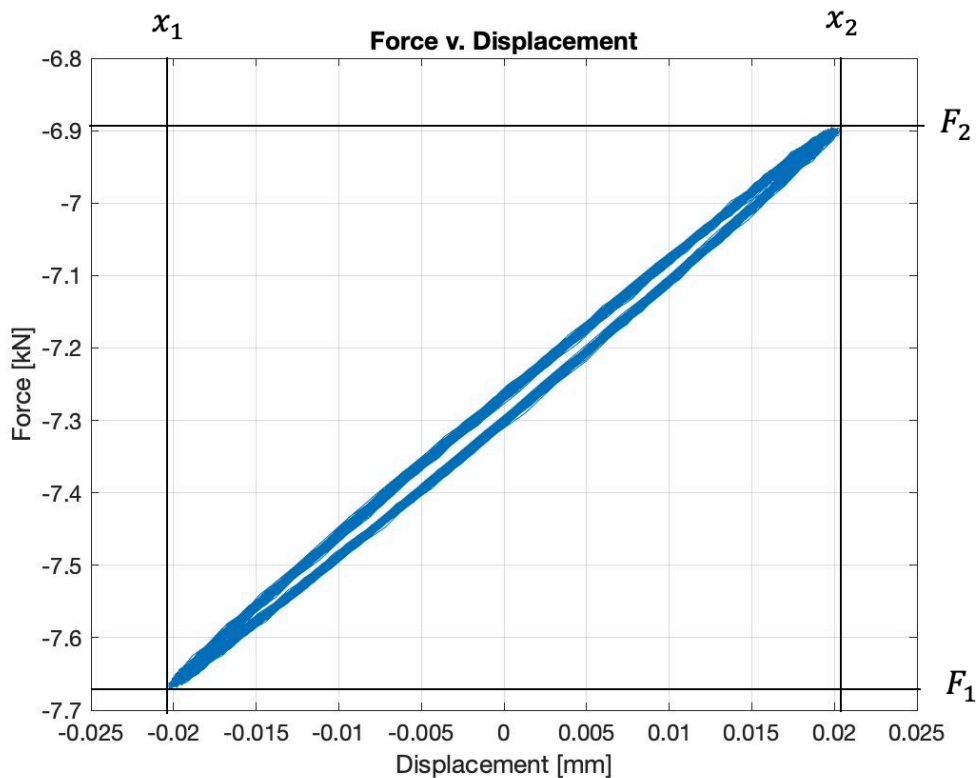
Figure 22: Example harmonic hysteresis loop

In the next section, the results of the case study are presented along with observations and clarification on the values obtained during the data collection. The setup calibration study is presented first, then the results from a static stiffness test on the M01 mount, followed by the equivalent dynamic stiffness results from both M01 and L01.

3 Results

In this section, the results of the case studies are presented, with comments regarding the setup calibration procedure and the calibration study presented first, followed by the presentation of static stiffness values from the M01 mount, and lastly followed by the equivalent dynamic stiffness results from the L01 and M01 mounts. The equivalent stiffness results are presented first in tabular format, then with respect to frequency, then to preload before presenting an isometric view to illustrate the combined effect. Relevant comments and observations are provided as needed to explain the presentation of results.

3.1 Setup calibration

The calibration study was performed over two days in May 2022 with assistance from the Aalto University Solid Mechanics Laboratory. On each testing day, a warm-up sequence of the load frame's hydraulic cylinder and inspection of equipment was performed upon entry to the lab. The equipment was within certified maintenance and calibration windows and no anomalies that would indicate equipment failure were noticed on any of the testing days. The loads induced by the machines were less than 25% of the maximum capable recording loads, and there were no signs of deflection or strain in the hydraulic equipment.

The installation sequence was as follows; install adapters onto mount until hand tight, adjust the jaw alignment brackets to accommodate the adapter width and length, insert mount into fixture, clamp lower pneumatic jaw, align into top jaw, clamp into top pneumatic jaw while under force control, perform inspection to ensure alignment is achieved. This was performed each day and subsequent inspection of the hardware for witness marks of damage were performed upon removal at the end of each test day.

The data collection method was under development during the calibration study to find out what the most effective model for gathering reliable data quickly and having repeatable results. This resulted in the first tests having a procedure to return to the zero preload (unloaded state) in between each frequency of oscillation in case there were memory effects with deflection of the rubber material. It was determined later that signal drift was a large factor in speed of data collection and an experiment was performed. A sweep from low to high frequency while keeping the mount at a given preload was the most effective method to collect multiple data points without waiting for the force values to settle. This was implemented in the later equivalent stiffness studies, but for the calibration study, post-processing of the data to remove drift was required.

The equivalent dynamic stiffness as calculated from the calibration study of the M01 mount is show in Table 7 below; the values are given in kN/mm and are sorted by preload value and frequency of oscillation.

Table 7: Stiffness results of calibration study for M01 mount

	5.0 Hz	**10.00 Hz**	**20.00 Hz**	**25.00 Hz**
4.50 kN	10.980	11.554	11.841	12.327
2.50 kN	10.917	11.924	11.709	12.240
0.00 kN	10.715	10.998	12.497	12.264
-2.50 kN	10.272	11.030	11.969	9.999
-5.00 kN	8.141	9.656	10.417	7.310
-7.50 kN	-	8.032	8.385	8.254
-9.50 kN	9.931	9.604	9.751	9.902

The maximum value of the equivalent stiffness is 12.497 kN/mm and occurs at 0.00 kN preload and 20.00 Hz oscillation frequency. The minimum value is 7.310 kN/mm and occurs at -5.00 kN preload and 25.00 Hz oscillation frequency and all the amplitudes of oscillation are 0.02mm. This data appears that as frequency increases for tensile loads, the stiffness increases and as frequency increases for compressive loads, the stiffness decreases.

The equivalent stiffness for the calibration study is plotted as a function of vibration frequency and shown in Figure 23 below. The red lines indicate tensile loads, blue- the zero-preload case, and black lines indicate compressive loads. The preloaded values are displayed at right with units of [kN].
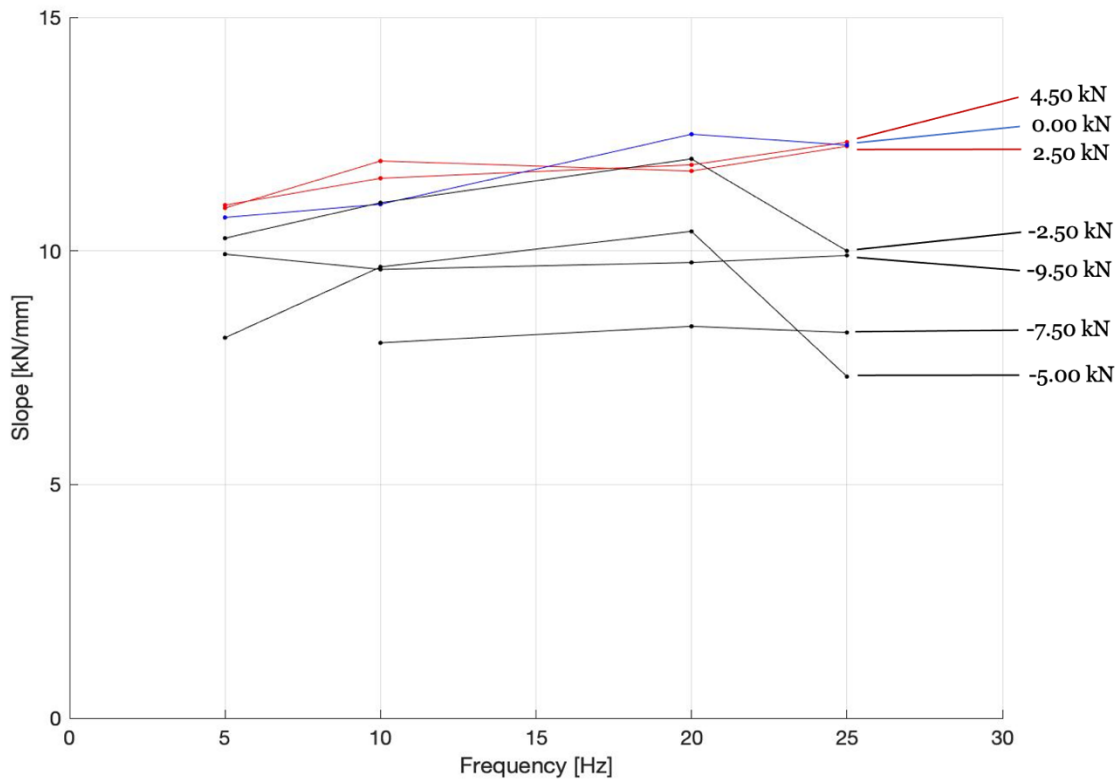
Figure 23: Calibration results M01 stiffness plot v. frequency

Slope with respect to oscillation frequency was a relationship of interest to the scope of the thesis, and trends that appear to relate to frequency shifts should be apparent on this chart. It appears there is not a strong correlation to the change in frequency for each preload value, and there are also not strong relations between compressive preloads and tensile preloads.

In this portion of the testing, the 7.50 kN compressive load case was not tested at 5.0 Hz due to an error with the transfer of the data file, but it was not deemed an issue because successive testing was planned that would include this in the next series of tests.

Figure 24 below displays the slope of M01 as a function of preloaded value, with the frequency of oscillation shown on the right side of the plot. The behavior of the mount with respect to stiffness appears to have more reactivity to preload than frequency, due to the trend of most of the data following a similar curve.
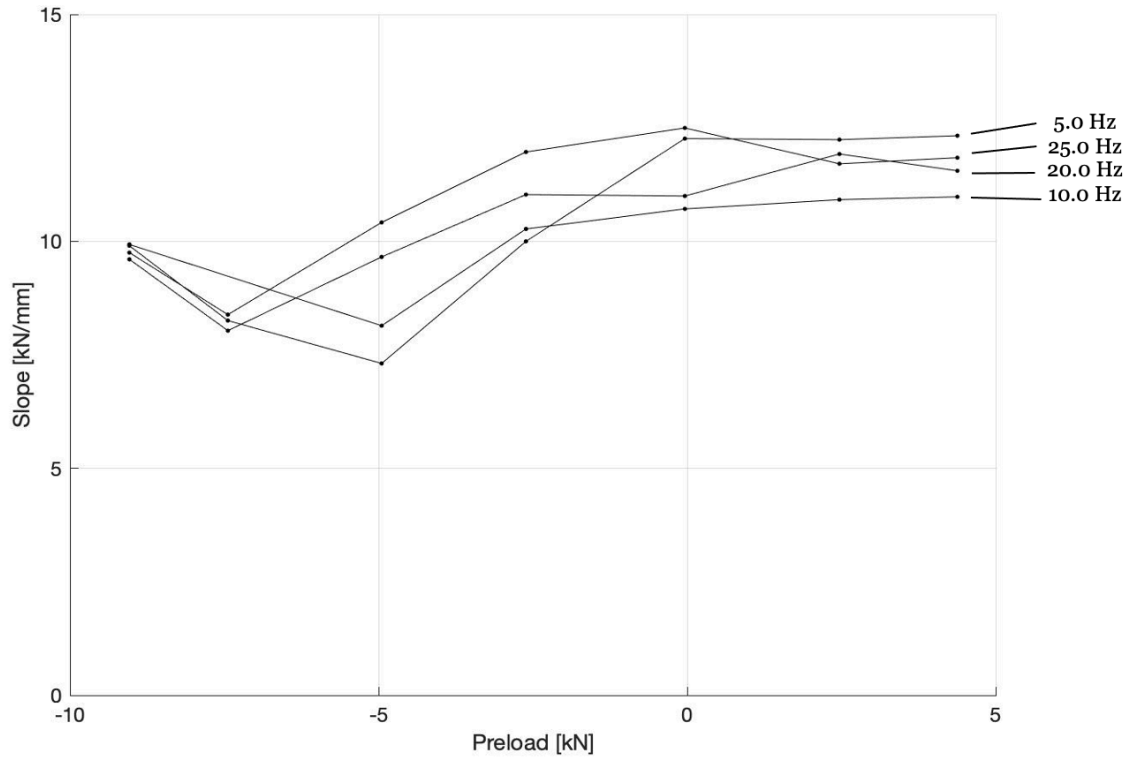
Figure 24: Calibration results M01 stiffness plot v. preload

This view shows that with higher compressive loads i.e. more negative, the equivalent stiffness is decreased and with higher tensile loads (more positive), the equivalent stiffness is increased. The context is that with a higher tensile preload the amount of effort to move the mount is increased with respect to the amount of effort to move the mount with a higher compressive preload.

Figure 25 below shows an isometric view of the slope versus frequency and preload and further helps to visualize the behavior of the M01 mount over the range of values tested during the initial stages of the work.
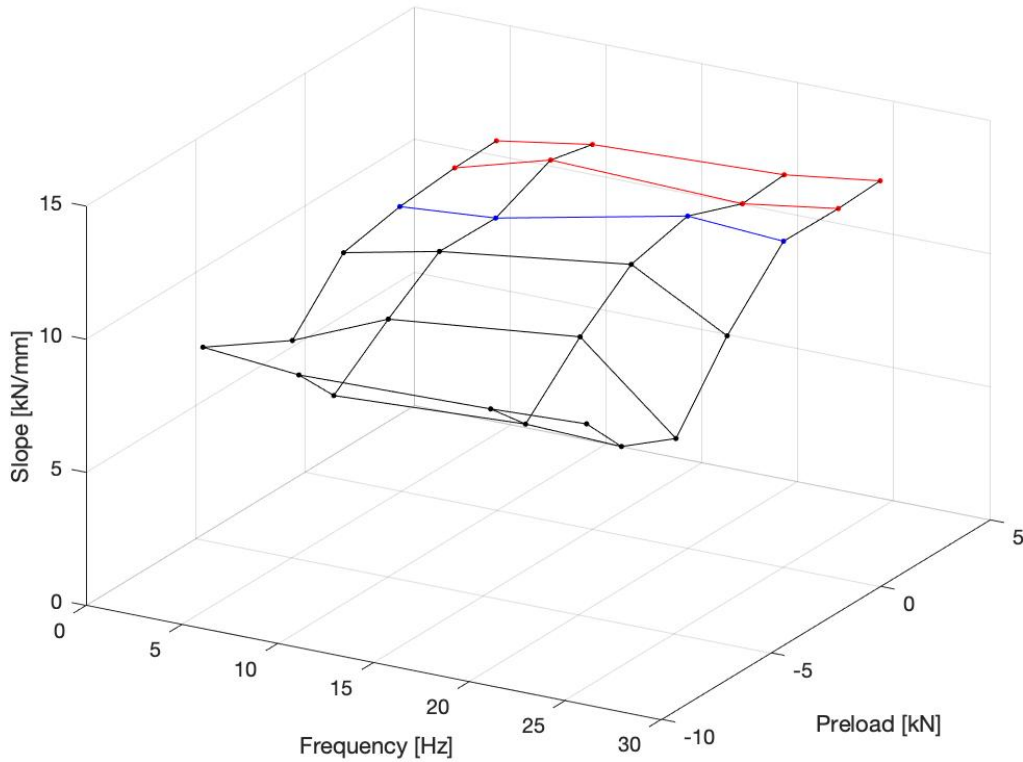
Figure 25: Calibration results M01 stiffness plot combined

The significant observations from the calibration study were as follows; the data can be manipulated to remove sources of drift, it is possible to determine interactions between different preloads and oscillation frequencies, and the data collection methods can be improved to allows for better and more characterization of the flexible mounting devices.

The next section briefly mentions the static stiffness of the M01 mount which was determined using a small amplitude deflection to determine a comparative baseline for the more rigorous equivalent dynamic stiffness calculations in section 3.3.

3.2 Static stiffness of M01 mount

The static stiffness of the M01 mount at zero preload is shown to be approximately 10.28 kN/mm with an R^2 value of 0.989. This value is calculated by starting with 0.00 kN preload and increasing the amount of force experienced by the mount by 100 N, allowing the reading to stabilize, then recording the corresponding displacement value in millimeters. Figure 26 below shows the data points plotted in MATLAB with the red values in tension, and black values in compression.
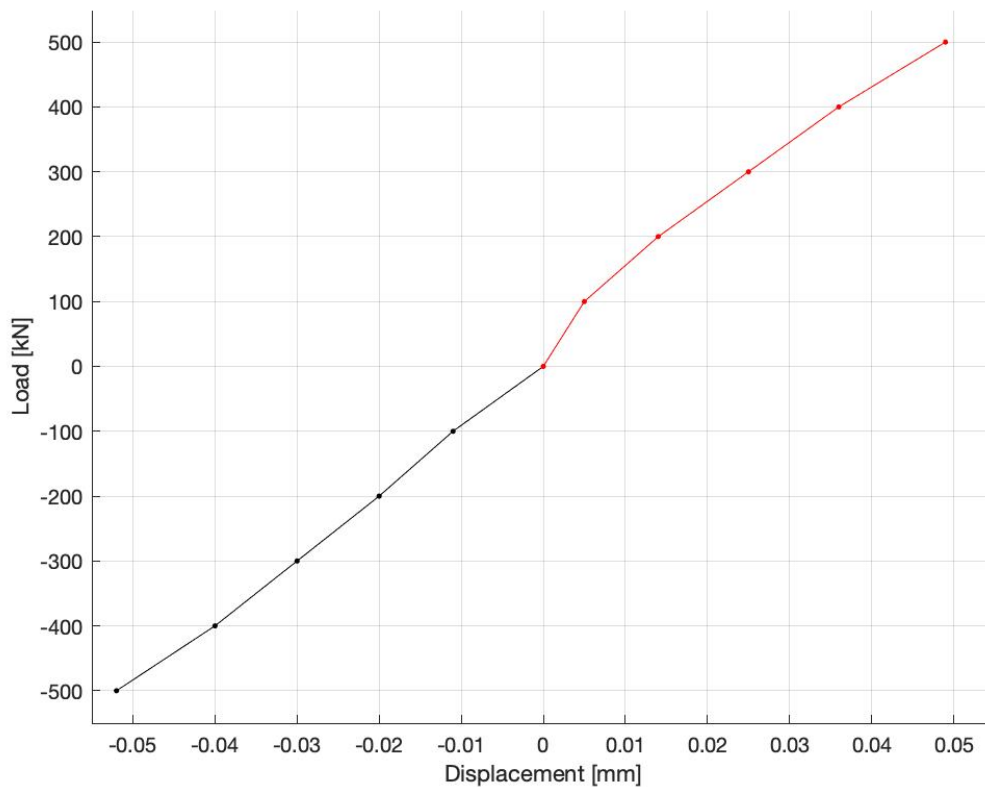
Figure 26: Static stiffness graph for M01 mount

This approximated stiffness is known to not be entirely accurate due to hysteresis (see Figure 6) and the properties of rubber mounts that involve higher order approximations when the elongation is larger. For the purposes of this thesis, the static stiffness was an intermediate result that was used to ensure the equipment would be able to impart the correct loading conditions and remain mechanically sound.

3.3 Dynamic stiffness of M01 mount

The equivalent dynamic stiffness for the M01 mount is presented in the tables and figures below. Table 8 below shows the equivalent stiffness values in kN/mm and are sorted by preload value and frequency of oscillation. These values were calculated using the updated data collection methods and believed to be an accurate representation of the flexible mount under the specified loading conditions.

Table 8: Equivalent stiffness table M01 mount – values in [kN/mm]

	1.0 Hz	2.5 Hz	5.0 Hz	7.5 Hz	10.0 Hz
7.50 kN	6.833	6.996	7.161	7.263	7.372
5.00 kN	9.839	10.146	10.375	10.524	10.680
0.00 kN	10.016	10.279	10.502	10.705	10.796
-2.50 kN	9.318	9.663	9.949	10.151	10.277
-5.00 kN	5.645	5.871	6.011	6.170	6.229
-7.50 kN	7.442	7.663	7.663	8.023	8.174
-9.00 kN	9.970	10.431	10.404	10.615	10.689

	12.5 Hz	15.0 Hz	17.5 Hz	20.0 Hz
7.50 kN	7.401	7.408	7.494	7.563
5.00 kN	10.772	10.856	10.928	10.995
0.00 kN	10.868	10.973	11.107	11.170
-2.50 kN	10.340	10.427	10.513	10.585
-5.00 kN	6.305	6.396	6.369	6.491
-7.50 kN	8.185	8.238	8.304	8.438
-9.00 kN	10.779	10.944	10.997	11.088

The stiffness values for the M01 mount have a maximum value of 11.170 kN/mm at 0.00 kN preload with 20.0 Hz vibration frequency, and minimum value of 5.40 kN/mm at 5.645 kN preload in compression with 1.0 Hz vibration frequency and all the amplitudes of oscillation were at 0.02mm.

The stiffness values are plotted as a function of frequency in Figure 27 below; the preload values are shown at right and the red lines indicate a tensile load, blue indicates zero-preload, and black lines indicate compressive loads.
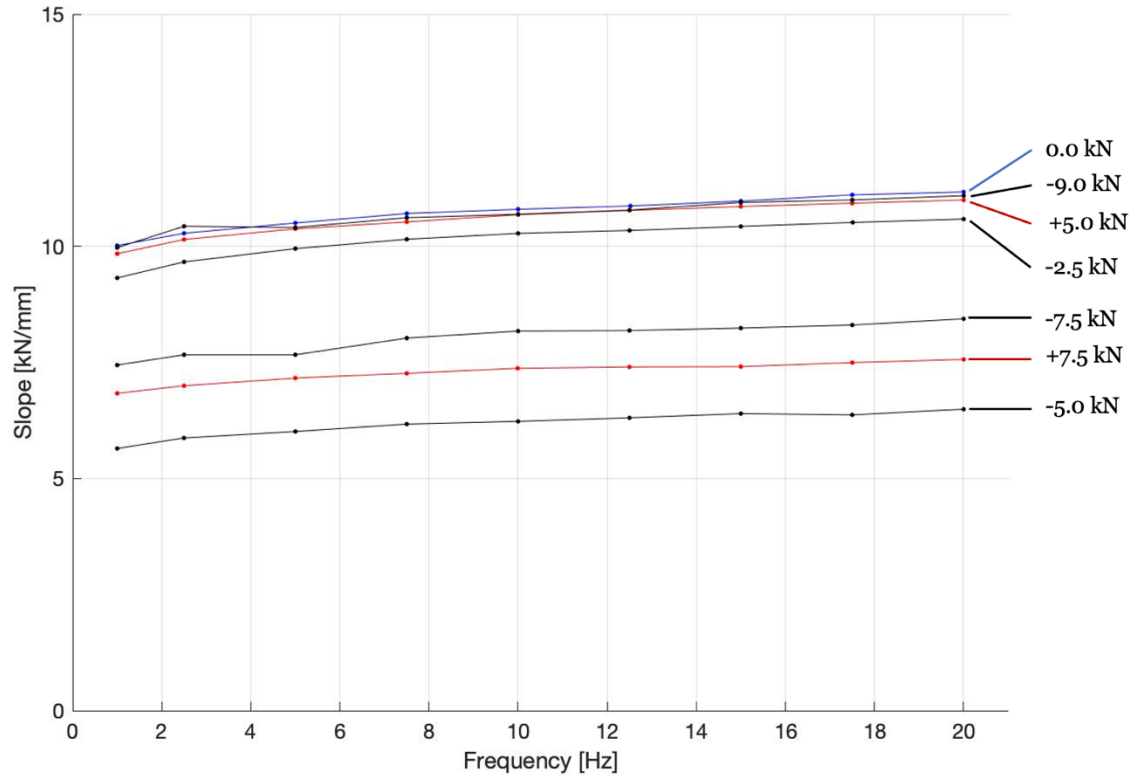

Figure 27: M01 stiffness plot v. frequency

All preload values tested in this study showed a similar increase in equivalent stiffness as the frequency of oscillation increased from 1.0 Hz to 20.0 Hz. One might expect the Mullin's effect to create strain softening of the mounting device, but since the amplitude is only 0.02mm this does not appear to influence the performance [7].

The equivalent dynamic stiffness is plotted as a function of preload value in Figure 28 below. The frequency of oscillation is indicated on the right-hand side of the figure with values ranging from 1.0 – 20.0 [Hz].
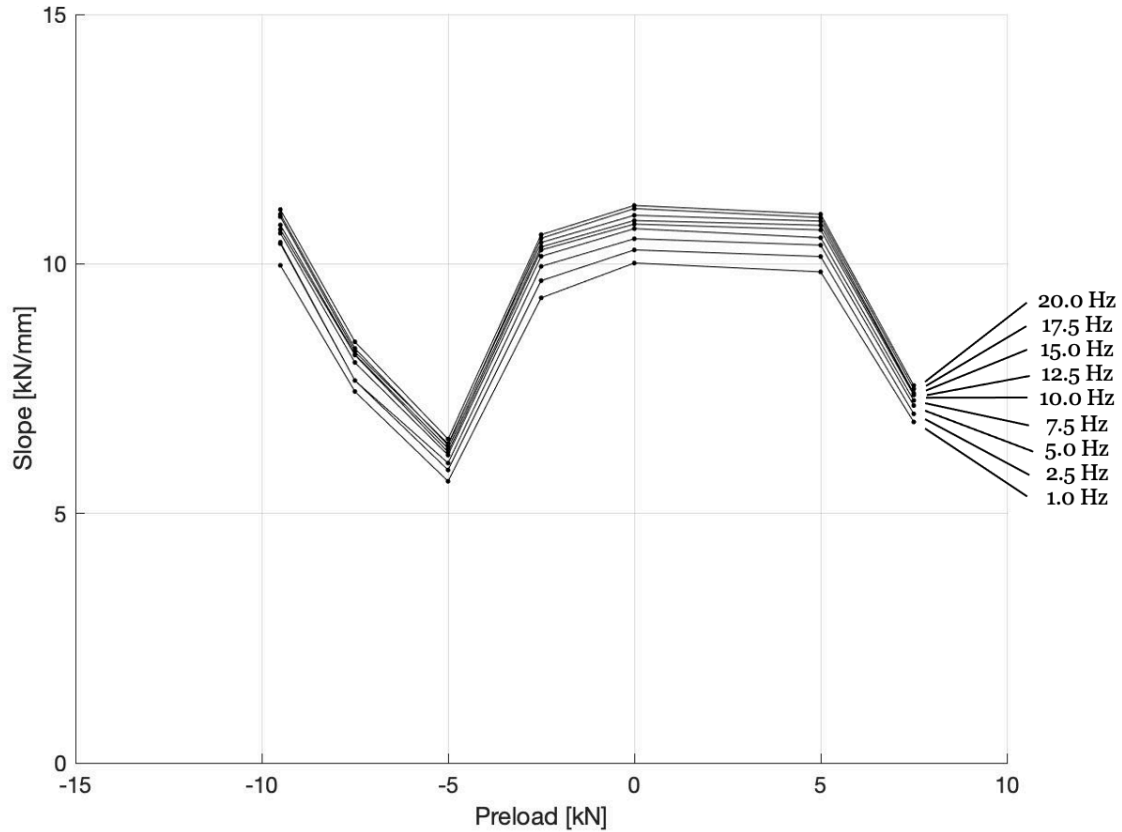
Figure 28: M01 stiffness plot v. preload

It is apparent that the shape of the slope is influenced more heavily by preload values, and only a minimal effect from the frequency of oscillation is observed. Additionally, the highest slope values at a given preload correspond with the highest frequency values, and the lowest slope values correspond with the lowest frequency values.

Figure 29 below shows the isometric view of the equivalent stiffness as a visualization aid. The preload parameter appears to have a larger effect on the equivalent dynamic stiffness than the frequency terms for the values tested in this study. This behavior is better illustrated in Figure 28, but this view shows how much more reactive to preload the slope value is than to frequency shifts.
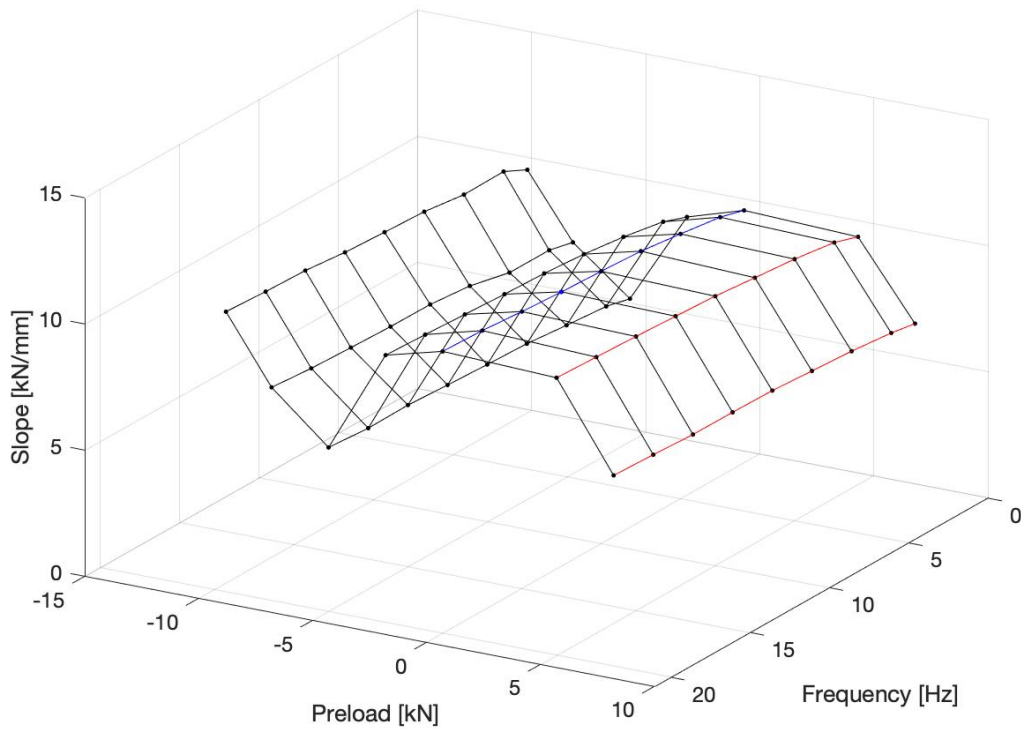
Figure 29: M01 equivalent stiffness - isometric view

A further observation is that at a given frequency, the equivalent stiffness will shift semi-predictably with increase in oscillation frequency and there is a larger difference with changing preload- namely from positive (tensile) to negative (compression). This is significant because in the loading scenario of marine environments, hogging and sagging loads often impart large swings which could induce a large stiffness change to the loaded element, albeit only for a brief time.

Following the display of stiffness data from the calibration study on the M01 mount, a comparison is made here to determine whether the data collection methods were similar. Figure 30 below is the plot of slope as a function of preload for the M01 mount with the values in the dashed black line taken from the calibration study and the solid black line values taken from the optimized collection method study. The frequency of oscillation is displayed at right for each set of data. The data from other non-matching frequencies is not displayed to increase the clarity of the information.
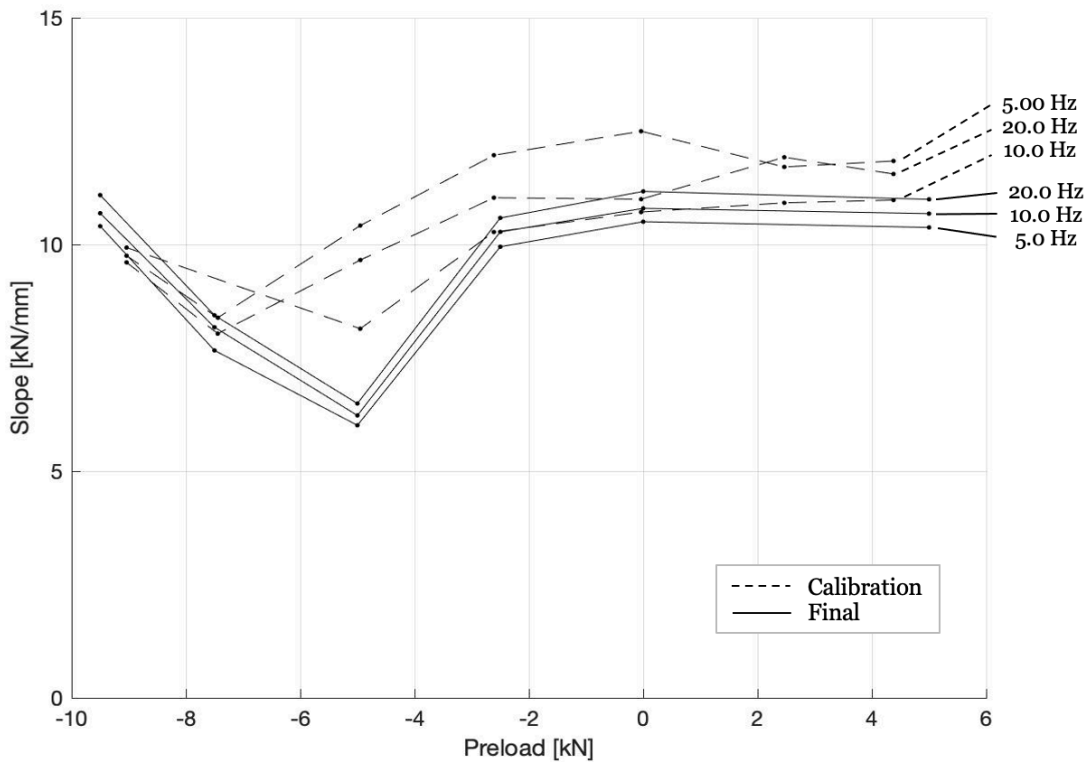
Figure 30: Comparison of M01 stiffness from calibration to final data collection

There seems to be general agreement to the values from each study except for at -5.0 kN compression, which could be an artifact of the testing method or something characteristic of the fibers of the rubber inside of the mount [9]. If the compression caused a larger percentage of fibers to be in contact at this preload with each other the stiffness could increase, which could result in a change in value due to the final stiffness study dwelling at that same compression and loosening the fibers at other oscillation frequencies. Further testing is required to determine if there is truth to this observation.

The next section presents the equivalent dynamic stiffness of the larger L01 mount in the same manner as the M01 mount and offers similar observations regarding behavior observed and later to be discussed.

3.4 Dynamic stiffness of L01 mount

The stiffness values for the L01 mount are shown below in Table 9 and have a maximum value of 41.63 kN/mm at 22.50 kN preload in compression with 20.0 Hz vibration frequency, and minimum value of 14.91 kN/mm at 7.50 kN preload in tension with 1.0 Hz vibration frequency. The L01 mount was tested at six different preloads with nine different frequencies of oscillation at each. Duplicate readings were taken to verify accuracy during the range of testing and have been normalized in this table.

Table 9: Equivalent stiffness table L01 mount

	1.0 Hz	**2.5 Hz**	**5.0 Hz**	**7.5 Hz**	**10.0 Hz**
15.00 kN	15.316	15.402	15.627	15.757	16.059
7.50 kN	15.715	16.470	16.422	16.518	16.595
0.00 kN	21.933	22.144	22.368	22.525	22.644
-7.50 kN	17.956	18.319	18.527	18.758	18.937
-15.00 kN	27.778	28.260	28.507	28.673	28.986
-22.50 kN	39.486	40.050	40.513	40.542	40.639

	12.5 Hz	**15.0 Hz**	**17.5 Hz**	**20.0 Hz**
15.00 kN	15.910	15.981	15.938	15.972
7.50 kN	16.689	16.733	16.870	16.920
0.00 kN	22.794	22.965	23.098	23.236
-7.50 kN	19.042	19.020	19.086	19.674
-15.00 kN	28.841	28.943	29.144	28.897
-22.50 kN	40.892	40.942	41.096	41.107

The stiffness values for the L01 mount have a maximum value of 41.107 kN/mm at -22.50 kN preload with 20.0 Hz vibration frequency, and minimum value of 15.316 kN/mm at 15.00 kN preload in tension with 1.0 Hz vibration frequency and all the amplitudes of oscillation were at 0.02mm.

Figure 31 below is a plot of the stiffness as a function of frequency of oscillation, the preload values are shown at right and the color of the lines indicate whether it is tensile (red), compressive (black), or neutral (blue).
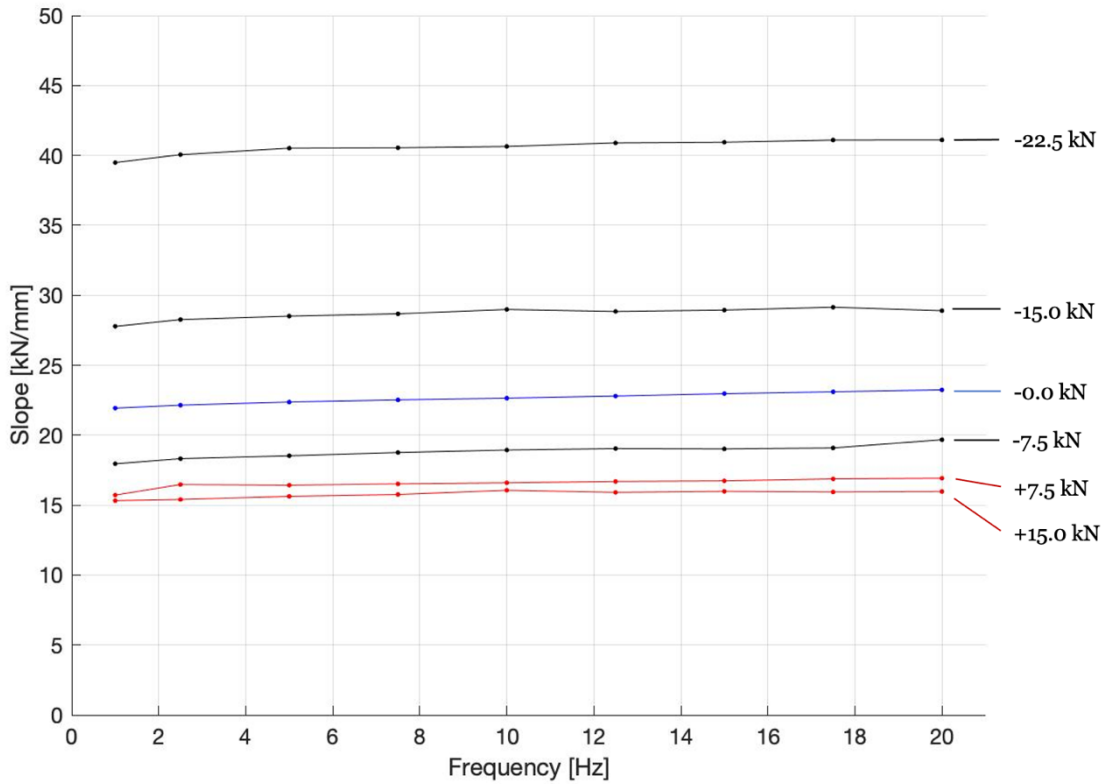
Figure 31: L01 stiffness plot v. frequency

The behavior of the equivalent stiffness around the neutral loading condition is of note because at 7.5 kN compression and 7.5 kN tension, the value of stiffness is less than the zero point and may indicate that the internal structure has a resonance when the strands are compressed or held in tension at the previously mentioned loading conditions.

Figure 32 is the plot of stiffness as a function of preload value for the L01 mount. The frequency values are shown at right and each line represents one frequency over the varied preloads. For high compression loads, there could be the effect of the metal casing internal to the mount that is causing a higher stiffness and further compression would lead to deflection of the metal instead of just rubber.
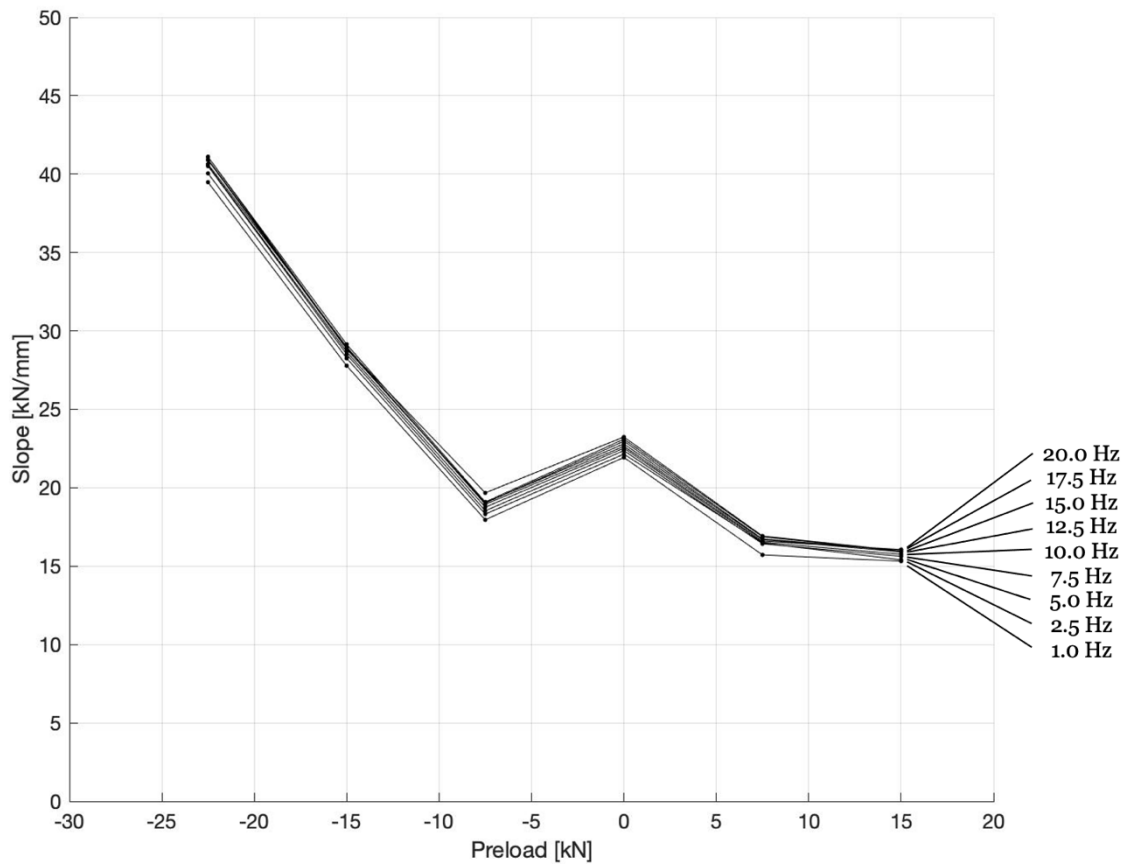
Figure 32: L01 stiffness plot v. preload

The equivalent stiffness varied most from -22.50 kN compression to 15.0 kN tension in which the value was more than 50% reduced in value during this transition. The characterization of this behavior is significant because depending on the installation location of the mount and whether it is subjected to higher tension than compression it could offer completely different damping and stiffness properties.

Figure 33 below shows an isometric view of the L01 stiffness values as a function of preload and frequency for a visualization aid of the numerical results regarding the behavior of the mount under certain loading conditions.
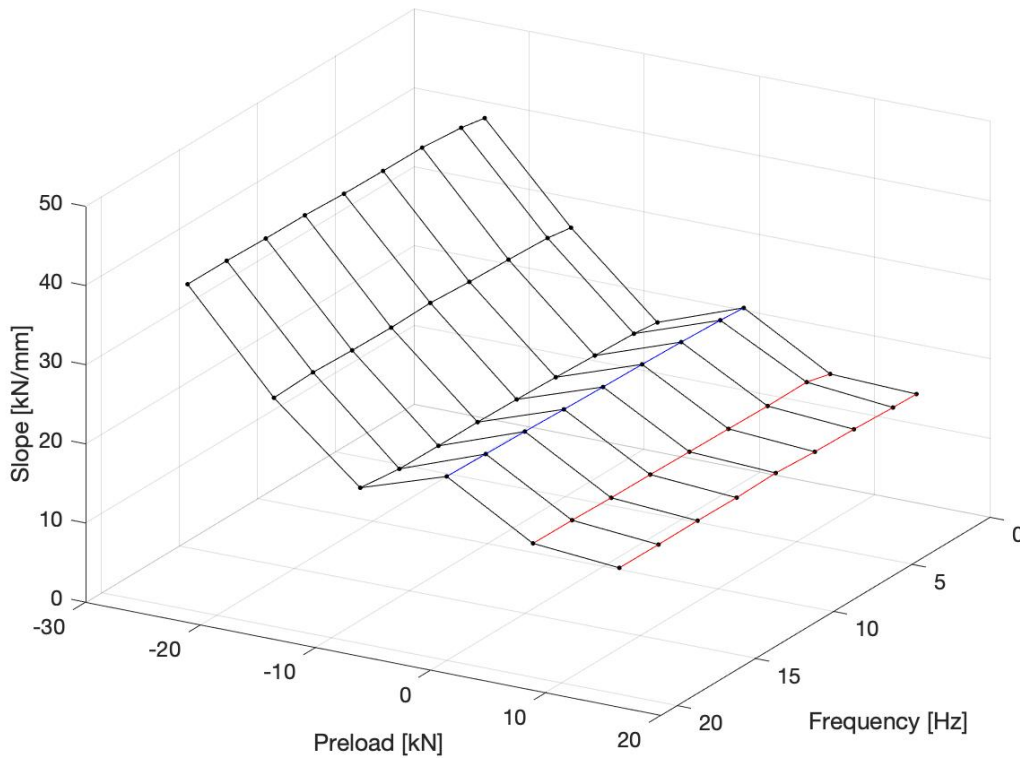
Figure 33: L01 isometric view of slope v. frequency and preload

Observation of the trends appears again that with preload changes there are more drastic effects to the equivalent stiffness of the mount, and at a given preload, an increase in frequency brings an increase in stiffness. The behavior around the zero-preload case appears to by symmetrical and could be attributed to the fiber behavior matching at each of the preloads and resulting in equal equivalent stiffness values [9].

The next section is the discussion section, where significant results and observations from the thesis work are presented. Additionally, sources of error and uncertainty are presented and comparisons to available literature are presented.

4 Discussion

In this section, the most significant results from the data analysis are reiterated to convey the importance of what was discovered in this thesis work. The equivalent stiffness values of the two different size mounts are compared and discussed what the differences observed were, the effect of amplitude on the equivalent stiffness is presented and discussed, and the context and significance of results are presented along with sources of error and comparisons to available literature information.

4.1 Significant results from data analysis

In Figure 34 below, the equivalent stiffness value and preload as a percentage of the respective maximum mount rating is plotted for comparison purposes. These normalized preload values allow for trends to be evaluated with respect to the amount of absolute load that is theoretically possible to impart on the flexible mounts.
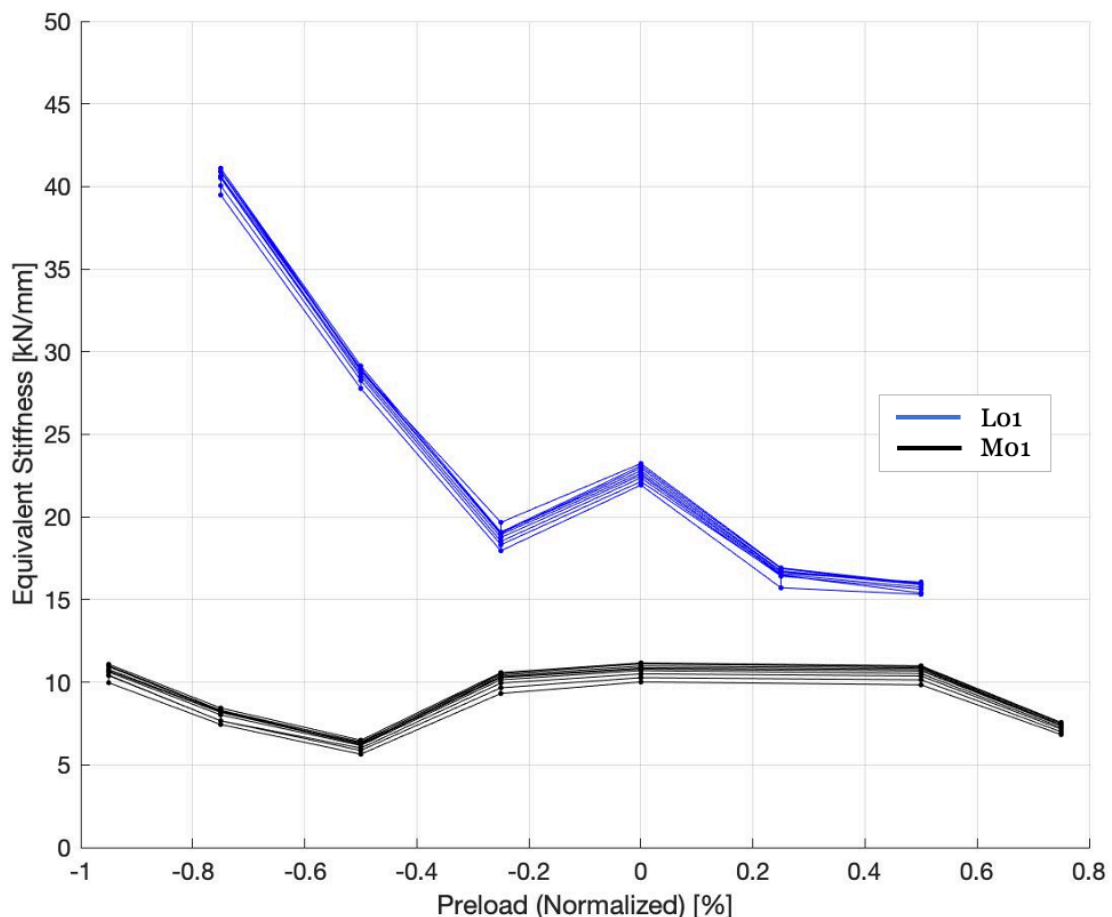
Figure 34: Normalized equivalent stiffness – comparison

The first observation is that for mounting devices they appear to be made of different materials or have fillers that change the stiffness properties significantly. The L01 mount is expected to have a higher stiffness due to the rating from the manufacturer, and the M01 mount to have lower stiffness but the characteristic curve

differences were not anticipated (see next observation). This could be attributed to the internal geometry of the mounts and interface surfaces to the metal support structure.

Further study could include repeating the same tests on duplicate mounts to determine if there is variation from mount to mount and also in between setup events. Due to the schedule of testing, only one replicate of each mount was tested and used to develop the testing method, but the intention is that multiple mounts use the adapters and generate comparative data to inform the design process. Another area of further study is dissecting the mounts to reveal any subjective differences between the mounts and identification of the materials. Another observation is that the L01 mount appears to be approaching a near asymptotic increase in equivalent stiffness which could be explained by the rubber fibers being compressed to their max within the mount geometry and the steel is directly loading steel to explain the large increase in stiffness. Both mounts are from the same manufacturer and used in similar applications and it seems counterintuitive that an asymptote could be approached when 75% of the compressive load is reached on one configuration and the other mount does not experience such a dramatic increase in stiffness.

The effect of an amplitude modification is displayed in Figure 35 below; the stiffness of the L01 mount at two different preloads is plotted as a function of frequency. The values in black indicate the 0.02mm amplitude which is the recommended large value of marine noise, and the red values are 0.04mm. The same test methods were used to calculate both, and it appears the behavior is similar with slight differences in slope magnitude.
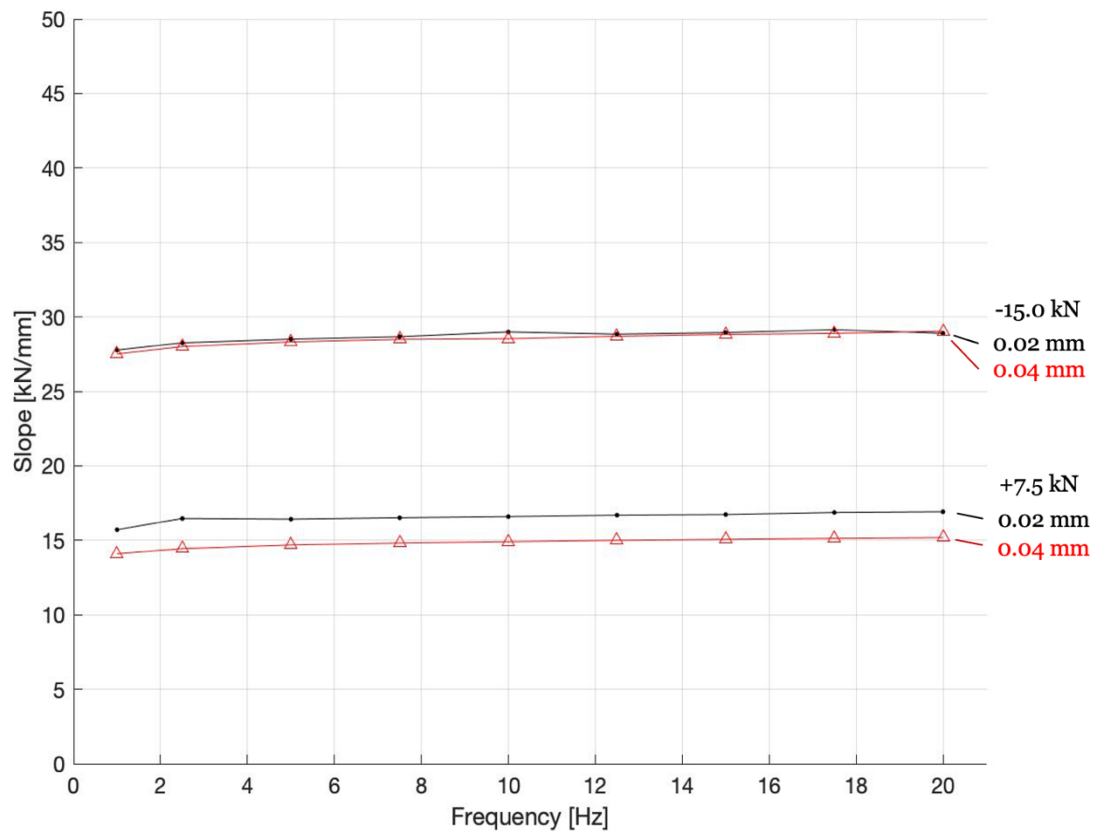
Figure 35: L01 mount slope effect of amplitude changes

Upon further reading regarding amplitude effects, the difference between these readings can be explained by the Mullins effect with the tensile load of +7.5 kN having a larger exacerbation of the straining as the fibers are not trapped within a steel structure and subjected to higher strain which results in less force required to deflect the material [7].

Figure 36 below shows the hysteresis effect due to amplitude changes and as the harmonic oscillation amplitude increases from 0.02mm to 0.04mm the hysteresis at the neutral preload value of 7.30 kN is increased from 0.002mm to 0.004mm.
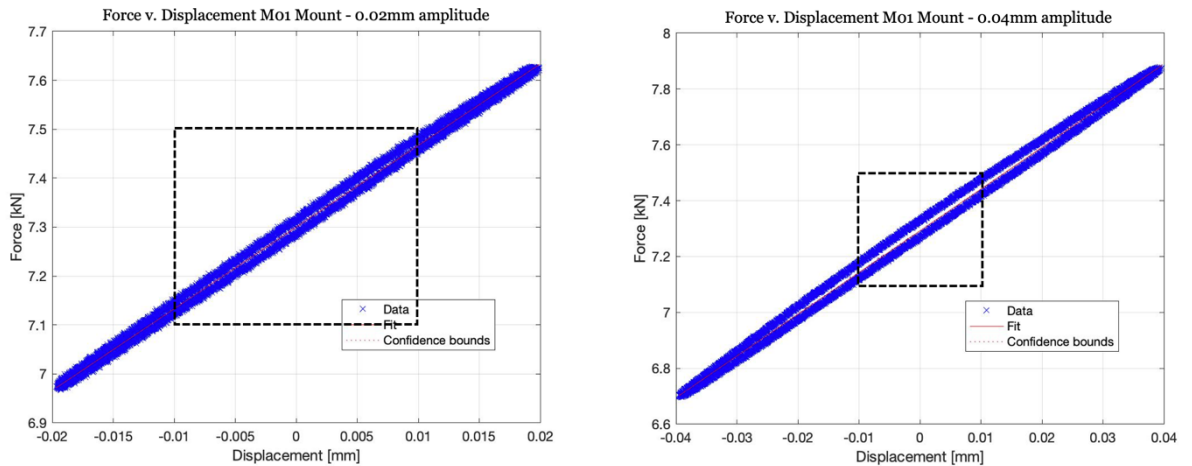
Figure 36: M01 Mount – 0.02mm and 0.04mm amplitude force v. displacement

The subsection indicated in black dashed line is the same size for both graphs in Figure 36 and are shown in more detail in Figure 37 with the hysteresis and slope indicated on each. The equivalent stiffness for the mount when the amplitude is 0.04mm is 14.69 [kN/mm] and when the amplitude is 0.02mm it is 16.41 [kN/mm].
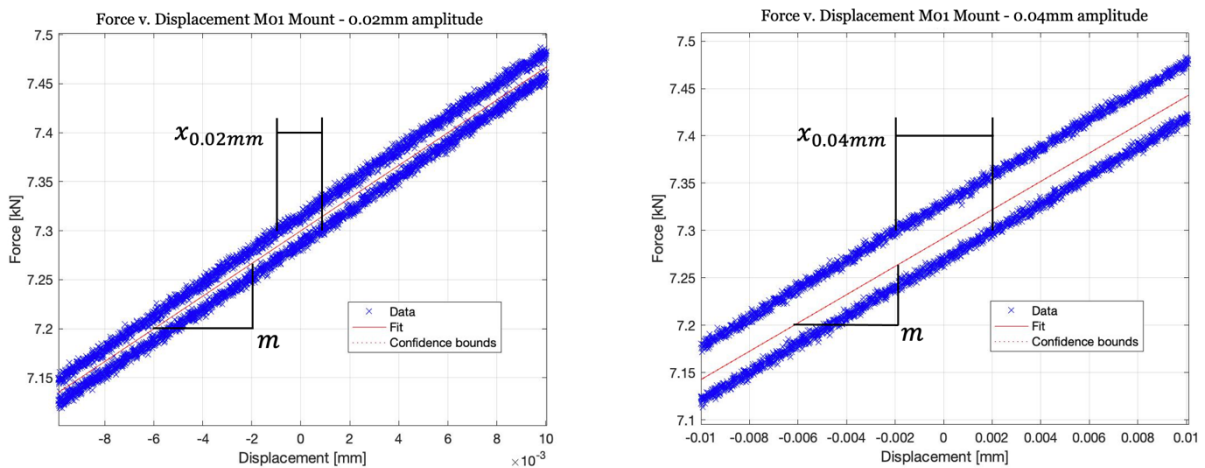
Figure 37: M01 mount – effect of amplitude on hysteresis and slope

This increase is logical due to the same frequency of oscillation, and when compared against literature and sources the critical amplitude is not near these values and the rubber internal friction behaves in the same manner [19]. If the increase in amplitude caused the hysteresis to increase or decrease in a non-linear manner, then the internal network of fibers would be likely the cause of such behavior [7].

4.2 Impact on marine structural design

The equivalent stiffness values of the two mounting devices are shown to be affected by preload more than frequency of oscillation. The interpretation of this behavior is that the hogging and sagging load values of the marine environment will affect how well the mount performs in both iterations of the devices more than the changes to vibration frequency. The mounts of this nature will need to be installed in a predictable loading window and if there are changes to the direction of force, the equivalent stiffness could change by more than 25%. If the mount is installed in a location where it does not have large changes in preload value, the vibration frequency changes would have minimal effect on the performance of the flexible mount. This mount could be utilized in a scenario where the preload value is light, or always in tension up to 50% of the maximum load rating. This would allow for prediction of the equivalent stiffness and not cause large shifts in properties and potential changing of principle natural frequencies. This could also be advantageous to the marine engineer with the ability to tune the properties of the installed mounting devices through adjustment of the threaded rods following sea trials or other post-installation testing. Further testing is required to determine if this type of mount can reduce proliferation of noise in the marine environment as the focus of the testing was equivalent stiffness and not damping. Combined loading and additional factors such as temperature and material modifications would also be required to perform a thorough analysis prior to utilization in a new design.

The main sources of error and uncertainty in this thesis are due to the low number of test runs performed to obtain the equivalent stiffness data. There were several loading scenarios that had multiple readings taken and had general agreement, but it is not adequate to inform a vibration study based on these calculations alone. To improve the reliability of the equivalent stiffness values, more tests at the same conditions are required and then statistical analysis performed to determine the probabilistic stiffness values should be performed. Additionally, the temperature and humidity in the laboratory were monitored but not modified to the same values, and with rubber materials, there is a dependence on these factors which should be further explored and controlled to fully characterize the behavior of the mounts.

The uncertainty in the values of this study is difficult to predict; the load frame is capable of reliably recording values to 10 significant figures and the results typically included three to five significant figures. The context of the results is more important than the miniscule differences between equivalent dynamic stiffness readings, meaning that when the mount is used in compression it could have nearly double the stiffness properties than when the same mount is used in tension even though the oscillation frequencies are the same.

5 Conclusion

Based on a literature review regarding flexible mounting solutions for both land and marine-based systems was conducted, applicable published studies and works were reviewed to determine methods of analysis and general best practices for these types of mounting devices. A practical case study was conceived, planned, executed, and reviewed during the study period of the thesis to better understand the important relationships between test parameters. It was discovered that preload conditions are more influential on the stiffness of these types of mounts than frequency of vibration. It was discovered that at a given preload value, the imparted frequency changes shifted the stiffness in a more predictable manner than preload modifications, but it is not obvious the direction they shift. The internal geometries of the mount features may have impacted the behavior and demands further study to continue the characterization effort.

The value of discovery in this thesis in context of similar work is that the predictions from the state-of-the-art behavior and measured values followed similar trends. The mount was not directly comparable to other types of rubberized mounts and future study is required to ascertain what effect the steel and other loading conditions had on the end results for each scenario. The provided flexible support systems were characterized with respect to the equivalent stiffness values in dynamic modes and as a function of preload values and vibration frequency inputs. The amplitude of oscillation was held constant for all trials except the last two runs and the impact to stiffness was noted, which requires further study to characterize this parameter. The data collection method was optimized to allow for follow-on testing with the same equipment and analysis methods.

Future lines of study include higher force loads, including values outside of the manufacturer's recommended maximum loads and higher and lower frequencies with combined effects of an input signal which has two modes of vibration, one with very low frequency of 0.10 Hz and amplitudes of 1.0 mm or more to mimic the hogging and sagging loads combined with higher frequencies of 5.0-20.0 Hz and amplitudes of 0.02mm to mimic the marine vibrations from engine and other outfitting equipment. Other types of mounting orientations and axes could be applied to the same test article to determine whether interesting behaviors exist within the same bounds of the study already completed. Additional types of mounts can and should be tested using the same test setup and procedure to determine whether there are characteristic differences between other available technologies. Further testing could be carried out utilizing the information and test methods presented in this thesis, and through this additional testing the usefulness of the data from a practical design standpoint is increased.

The solutions to flexible structures in ship- and land-based constructions consist of rubber elements that are either combined into the material as a filler which modifies the properties of the composite, cast into shapes which allow for adequate stiffness and damping properties between masses, and carefully installed around a perimeter frame to provide minimal translation of forces and vibrations to the surrounding bodies. The different test methods for assembly structure elements must be developed through understanding of the purpose of each element. For example, the unit under test is rigidly installed between a large marine exhaust pipe and the supporting walls of the ship, with very small vibrations at a known frequency spectrum. The test method developed mimicked the installed configuration in the load frame with both ends held together and the drive piston of the MTS induced vibrations into the mount which were recorded on the top end which simulated the actual load case. For other types of mounts the methods should be like how it is used and if it is not possible then combined effects could be considered.

From the data collected on the dynamic stiffness values in this body of work, it appears that the effect of preload has a larger impact on stiffness than the frequency of oscillation when the amplitude is held constant. This behavior did not create a predictable outcome for the mounts of different sizes, but from test to test, the impact on stiffness from changing the vibration frequency was measurable in the <10% range whereas preload was >100%. From the data collected in this study, the M01 mount and L01 mount have unique signatures in terms of dependence of stiffness on preload and vibration frequency and cannot be effectively scaled up or down to predict the behavior of a given loading scenario. Further analysis and characterization are required prior to definitively stating that something fundamentally different is occurring with the elements, but at this time it is not obvious why the differences exist.

Further questions raised during the study include the following: Does the effect of operating temperature change the characteristics and behavior of the mounting devices significantly? What effect does resonance frequency of the mount have with respect to stiffness, and can it be mitigated for a captive system? What impact does the internal structure of the mount have on mount characteristics and is it possible to tune dynamic stiffness through combined loading? What is the difference between duplicate mounts from the same manufacturer? How to characterize the equivalent stiffness of mounts with the same geometry but alternate materials of construction?

6 References

[1] D. Kerstetter, J. Xie ja A. Mattila, "The attributes of a cruise ship that influence the decision making of cruisers and potential cruisers," *International Journal of Hospitality Management*, pp. 152-159, 2012.

[2] Royal Caribbean, "Spectrum of the Seas Activity Overview," [Online]. Available: https://rccl-h.assetsadobe.com/is/image/content/dam/royal/data/activity/flowrider/spectrum-of-the-seas-flowrider-skypad-ripcord-activities.jpg?$750x667$. [Haettu 28 October 2022].

[3] Royal Caribbean, "Liberty of the Seas Amenities," [Online]. Available: https://www.tirun.com/cruise-lines/royal-caribbean-international/ships/img/liberty-of-the-seas/Liberty-Sports-Court.jpg. [Haettu 28 October 2022].

[4] TUI Cruises, "Mein Schiff 3 Amenities," [Online]. Available: https://img.welt.de/img/regionales/hamburg/mobile114117797/0262504367-ci102l-w1024/Tui-Cruises-Mein-Schiff-3-3.jpg. [Haettu 28 October 2022].

[5] V. Bertram, "Vibrations," tekijä: *Practical Ship Hydrodynamics*, Elsevier Ltd, 2012, pp. 205-239.

[6] I. Demir, A. Izadi ja M. Y. Javaid, "Experimental Study of Cabin and Engine Vibration Isolation Elements," Linnaeus University, Växjö, Sweden, 2011.

[7] Z. K. Laka and L. A. I. S. Coop., "Dynamic Stiffness and Damping Prediction on Rubber Material Parts, FEA and Experimental Correlation," London Metropolitan University, London, 2016.

[8] G. R. Reddy, H. P. Muruva ja A. K. Verma, "Introduction to Structural Dynamics 3 and Vibration of Single-Degree-of-Freedom Systems," tekijä: *Textbook of Seismic Design*, Springer, 2019, pp. 72-93.

[9] L. R. Treloar, "Chemical Constitution of Rubbers," tekijä: *Physics of Rubber Elasticity*, Oxford, Oxford University Press, 2009, pp. 1-23.

[10] J. Meggitt, A. S. Elliott, A. T. Moorhouse ja K. H. Lai, "In-Situ Determination of Dynamic Stiffness for Resilient Elements," *Institution of Mechanical Engineers, Part C: Journal of Mechanical Engineering Science*, 2015.

[11] L. Pust, L. Pesek, F. Vanek ja J. Cibulka, "Laboratory measurement of stiffness and damping of rubber element," *Engineering MECHANICS*, pp. 13-22, 2017.

[12] P.-E. Austrell, "Modeling of Elasticity and Damping for Filled Elastomers," Lund University, Lund, Sweden, 1997.

[13] T. Ramachandran, K. P. Padmanaban ja P. Nesamani, "Modeling and Analysis of IC Engine Rubber Mount using Finite Element Method and RSM," *Procedia Engineering 38,* pp. 1683-1692, 2012.

[14] F. Alkhatib, "Techniques for Engine Mount Modeling and Optimization," University of Wisconsin-Milwaukee, Milwaukee, 2013.

[15] M. Rahman, A. Al-Ghalib ja F. Mohammad, "Anti-vibration characteristics of rubberised reinforced concrete beams," *Materials and Structures,* pp. 1807-1815, 2014.

[16] SB Broneske, *Vibration Mounts & Expansion Bellows for the exhaust pipe system,* Wahlstedt, Germany: SB Broneske, 2010.

[17] MathWorks, "MATLAB R2022b Help Center," 2022. [Online]. Available: https://www.mathworks.com/help/matlab/ref/filter.html?searchHighlight=filter%20function&s_tid=srchtitle_filter%20function_1#buagwwg-2. [Haettu 17 December 2022].

[18] M. G. Tárrago, L. Kari, J. Vinolas ja N. Gil-Negrete, "Frequency and amplitude dependence of the axial and radial stiffness of carbon-black filled rubber bushings," *Polymer Testing 26,* pp. 629-638, 2007.

[19] F. Coren, "Durability of Rubber Components under Multiaxial Cyclic Stresses," Espoo, Finland, 2017.

7 Table of Figures
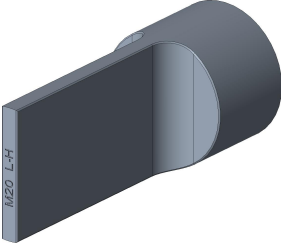
8   Appendix

8.1   Mounting adapter drawings

DRAWING NUMBER: M20_MOUNT_LEFT

DRAFTER: AARON KÖRKKÖ

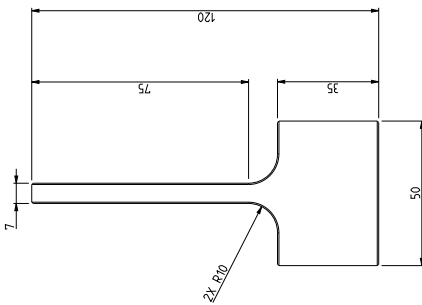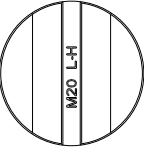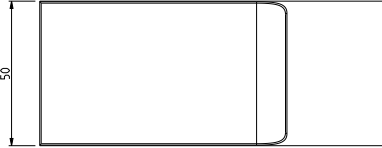DATE: 14 APRIL 2022

DRAWING NOTES:

1. MATERIAL: MILD STEEL BAR STOCK

2. SURFACE FINISH: CLEAN BURRS AND SHARP EDGES

3. PERMANENTLY MARK PART ON TOP SURFACE WITH "M20 L-H" AS SHOWN
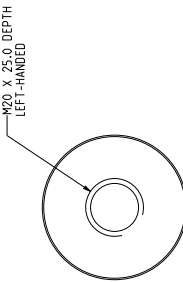   METHOD CAN BE LASER MARKING OR MACHINE MILLING OR EQUIVALENT

CHAMFER 0.5MM ALL AROUND

TAPER ANGLE IS REF ONLY
SIMILAR ANGLES ACCEPTABLE

M20 x 25.0 DEPTH
LEFT-HANDED

M20 L-H

120

75

35

50

50

7

2X R10

(210°)

16.6

25

DRAWING NOTES:

1. MATERIAL: MILD STEEL BAR STOCK

2. SURFACE FINISH: CLEAN BURRS AND SHARP EDGES

3. PERMANENTLY MARK PART ON TOP SURFACE WITH "M20 R-H" AS SHOWN
   NOTE: METHOD CAN BE LASER MARKING OR MACHINE MILLING OR EQUIVALENT

M20 R-H

120

75

35

50

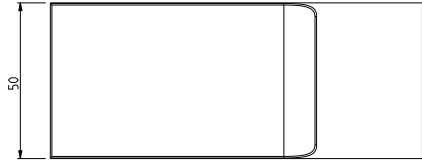2X R10
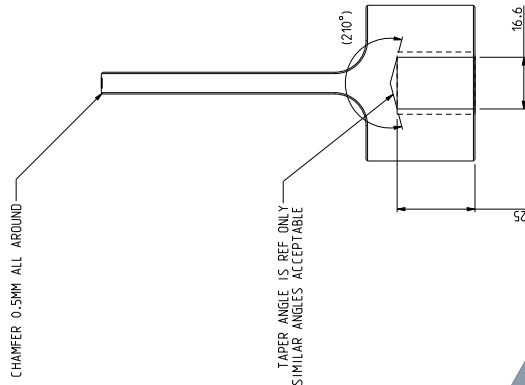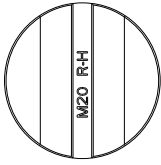
50

M20 R-H

M20 X 25.0 DEPTH
RIGHT-HANDED

(210°)

16.6

25

CHAMFER 0.5MM ALL AROUND

TAPER ANGLE IS REF ONLY
SIMILAR ANGLES ACCEPTABLE

DRAWING NUMBER: M20_MOUNT_RIGHT

DRAFTER: AARON KÖRKKÖ

DATE: 14 APRIL 2022

DRAWING NOTES:

1. MATERIAL: MILD STEEL BAR STOCK

2. SURFACE FINISH: CLEAN BURRS AND SHARP EDGES

3. PERMANENTLY MARK PART ON TOP SURFACE WITH "M24 L-H" AS SHOWN
   NOTE: METHOD CAN BE LASER MARKING OR MACHINE MILLING OR EQUIVALENT

M24 L-H

130

75

7

45

50

50

M24 L-H
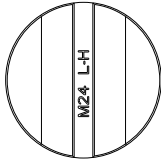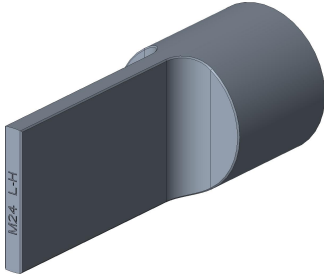
M24 X 3.0 PITCH X 35.0 DEPTH
LEFT-HANDED

CHAMFER 0.5MM ALL AROUND

(210°)

19.95

35

TAPER ANGLE FOR REF ONLY
SIMILAR ANGLES ACCEPTABLE

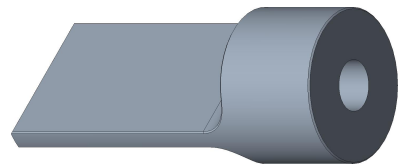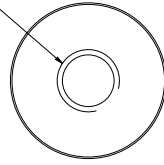DRAWING NUMBER: M24_MOUNT_LEFT

DRAFTER: AARON KÖRKKÖ

DATE: 14 APRIL 2022

DRAWING NOTES:

1. MATERIAL: MILD STEEL BAR STOCK

2. SURFACE FINISH: CLEAN BURRS AND SHARP EDGES

3. PERMANENTLY MARK PART ON TOP SURFACE WITH "M24 R-H" AS SHOWN
   METHOD CAN BE LASER MARKING OR MACHINE MILLING OR EQUIVALENT

CHAMFER 0.5MM ALL AROUND

(210°)
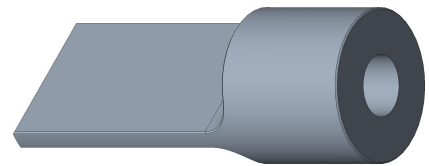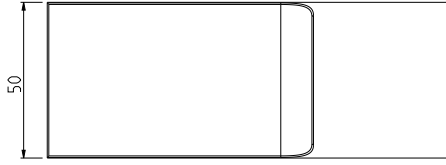
TAPER ANGLE IS REF ONLY
SIMILAR ANGLES ACCEPTABLE

19.95

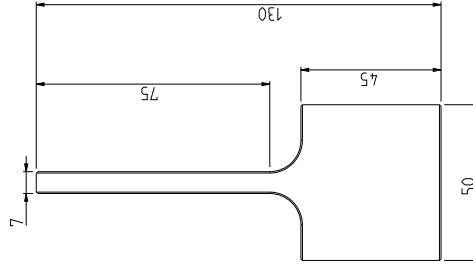35

130

75

45
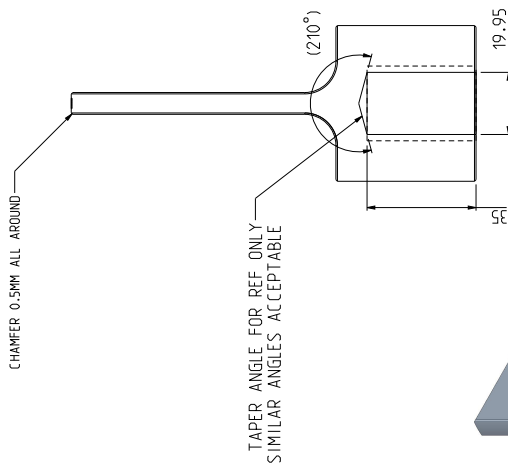
50

2X R10

50

M24 R-H
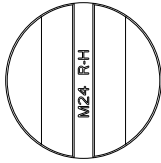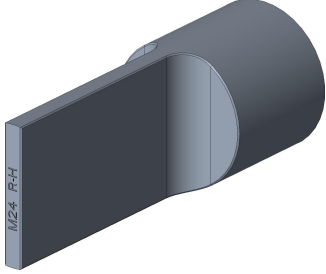
M24 x 3.0 PITCH X 35.0 DEPTH
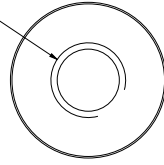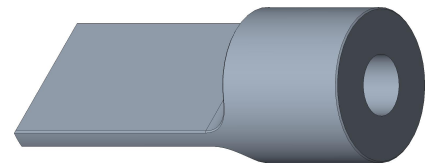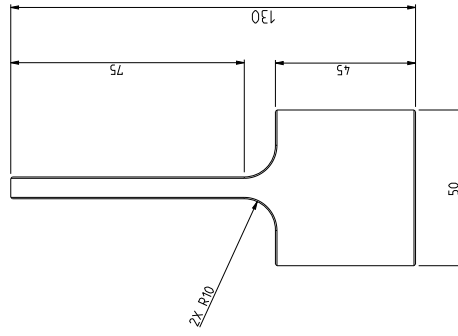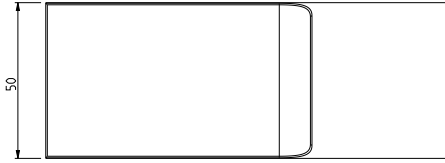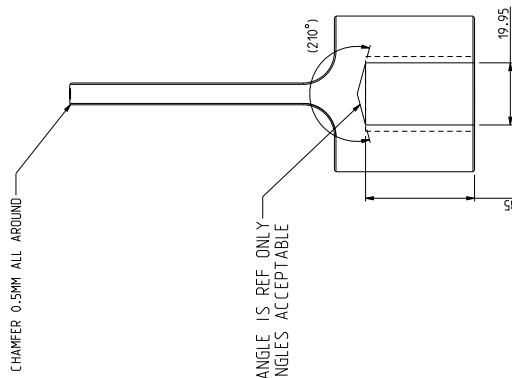RIGHT-HANDED
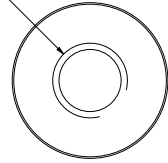
DRAWING NUMBER: M24_MOUNT_RIGHT

DRAFTER: AARON KÖRKKÖ

DATE: 14 APRIL 2022

8.2 MATLAB code

The MATLAB code presented in this section represents the data preparation and analysis tools used to create the values in the results and discussion sections in the main text. They are meant to be used in conjunction with the raw text files of the output data from the load frame to calculate the appropriate results. There are inputs within the text that are intended to be modified so they calculate the correct values and filter appropriately. The comments serve to help but may not be comprehensive for every section. The initial calibration study is presented first, then the equivalent dynamic stiffness study for the M01 mount, then the stiffness study for the L01 mount.

```matlab
%% Meyer Turku – Master's thesis workbook
%% Date: 28 December 2022 Name: Aaron Korkko
% Case Study #1 performed May 2022 on Broneske Mount M01
% close and clear variables
close all
clear
clc

test_num = 1;        %select the test number for data analysis
all_data = 0;         %set to 1 for all data in a test set, not subset

% Matrix of start and stop times for frequencies *manually entered*
timing_matrix = [2.5  140; 2.5   135; 5     300; 10    375; 5     100; 5
            70; 5       50;
5           52; 3     101; 5     100; 5     110; 2.5   105; 4     115;
5           100; 4    49; 4      49; 2.5    54; 4      52; 2.5    127.0;
3           121.0; 5  120.0; 5  120.0;
5           213.0; 50 261.0; 5  159.0; 5   145.0; 5   120.0; 10  155.0;
5           130.0;
5           170.0; 100 210.0; 5 145.0; 5   184.0; 5   191.0; 5   132.0;
5           118.0;
5           154.0; 5  131.0; 5  175.5; 5   197.0; 5   45.0; 5    120.0;
50          115.0;
50          124.0; 5  120.0; 5  120];

% Set variables to only look at desired portion of data – test specific
start_time = timing_matrix(test_num,1);
stop_time = timing_matrix(test_num,2);

% % Set variables to specific values of interest
% start_time = 20;
% stop_time = 80;

if all_data==1;
    start_time = 0;
    stop_time = 5000;
end

%test matrix with file names of all tests
test_names = ["1_preload_0kn_fc_ampl_500n_05hz.txt";
    "2_preload_-2.5kn_fc_ampl_500n_05Hz.txt";
```

```matlab
    "3_preload_-5kn_fc_ampl_500n_05hz.txt";
    "4_preload_-7.5kn_fc_ampl_500n_05hz.txt";
    "5_preload_-5kn_dc_ampl_002mm_5hz.txt";
    "6_preload_-5kn_dc_ampl_002mm_10hz.txt";
    "7_preload_-5kn_dc_ampl_002mm_20hz.txt";
    "8_preload_-5kn_dc_ampl_002mm_20hz_run_2.txt";
    "9_preload_-2.5kn_dc_ampl_002mm_10hz.txt";
    "10_preload_-7.5kn_dc_ampl_002mm_10hz.txt";
    "11_preload_-9.5kn_dc_ampl_002mm_10hz.txt";
    "12_preload_0kn_dc_ampl_002mm_10hz.txt";
    "13_preload_2.5kn_dc_ampl_002mm_10hz.txt";
    "14_preload_4.5kn_dc_ampl_002mm_10hz.txt";
    "15_preload_4.5kn_dc_ampl_002mm_20hz.txt";
    "16_preload_2.5kn_dc_ampl_002mm_20hz.txt";
    "17_preload_0kn_dc_ampl_002mm_20hz.txt";
    "18_preload_-2.5kn_dc_ampl_002mm_20hz.txt";
    "19_preload_0kn_dc_ampl_002mm_20hz.txt";
    "20_preload_-2.5kn_dc_ampl_002mm_20hz.txt";
    "21_preload_-5kn_dc_ampl_002mm_20hz.txt";
    "22_preload_-7.5kn_dc_ampl_002mm_20hz.txt";
    "23_preload_-9.5kn_dc_ampl_002mm_20hz.txt";
    "24_preload_4.5kn_dc_ampl_002mm_20hz.txt";
    "25_preload_4.5kn_dc_ampl_002mm_20hz_run_2.txt";
    "26_preload_2.5kn_dc_ampl_002mm_20hz.txt";
    "27_preload_2.5kn_dc_ampl_002mm_25hz.txt";
    "28_preload_0kn_dc_ampl_002mm_25hz.txt";
    "29_preload_2.5kn_dc_ampl_002mm_25hz.txt";
    "30_preload_4.5kn_dc_ampl_002mm_25hz.txt";
    "31_preload_-9.5kn_dc_ampl_002mm_25hz.txt";
    "32_preload_-7.5kn_dc_ampl_002mm_25hz.txt";
    "33_preload_-5kn_dc_ampl_002mm_25hz.txt";
    "34_preload_-2.5kn_dc_ampl_002mm_25hz.txt";
    "35_preload_-2.5kn_dc_ampl_003mm_25hz.txt";
    "36_preload_-2.5kn_dc_ampl_005mm_25hz.txt";
    "37_preload_-2.5kn_dc_ampl_008mm_25hz.txt";
    "38_preload_-2.5kn_dc_ampl_010mm_25hz.txt";
    "39_preload_-2.5kn_dc_ampl_014mm_25hz.txt"
    "40_preload_-2.5kn_dc_ampl_002mm_5hz.txt";
    "41_preload_-2.5kn_dc_ampl_002mm_1-20hz.txt";
    "42_preload_-5kn_dc_ampl_002mm_5hz.txt";
    "43_preload_-9.5kn_dc_ampl_002mm_5hz.txt";
    "44_preload_0kn_dc_ampl_002mm_5hz.txt";
    "45_preload_2.5kn_dc_ampl_002mm_5hz.txt";
    "46_preload_4.5kn_dc_ampl_002mm_5hz.txt"];

%loading of data from file selection
for i=1:length(test_names)
    if test_num == i
        file_name = test_names(i);
    end
end

%create variable arrays
array_data = readmatrix(file_name);
time = array_data(:,2);
force = array_data(:,3);
```

```matlab
disp = array_data(:,4);
count = array_data(:,5);

%% Cleaning up data section by removing NaNs, filtering, and windowing
%find NaNs inside of time matrix and remove related points
purge_t = find(isnan(time));
flip_purge_t = flipud(purge_t);
for i=1:length(purge_t)
    j=flip_purge_t(i);
    time(j)=[];
    force(j)=[];
    disp(j)=[];
    count(j)=[];
end

%find NaNs inside of force matrix and remove related data
purge_f = find(isnan(force));
flip_purge_f = flipud(purge_f);
for i=1:length(purge_f)
    j=flip_purge_f(i);
    time(j)=[];
    force(j)=[];
    disp(j)=[];
    count(j)=[];
end

%find NaNs inside of displacement matrix and remove all related data
purge_d = find(isnan(disp));
flip_purge_d = flipud(purge_d);
for i=1:length(purge_d)
    j=flip_purge_d(i);
    time(j)=[];
    force(j)=[];
    disp(j)=[];
    count(j)=[];
end

%smooth data by filtering
windowSize = 10;
b = (1/windowSize)*ones(1,windowSize);
a = 1;
force_f = filter(b,a,force);
disp_f = filter(b,a,disp);

% high pass filter implementation
fs = 200;
force_filt = highpass(force_f,0.5,fs);
force_filt = force_filt+mean(force_f);

%plot filtered v. raw signal
figure('Name','Noise Removal v. High Pass Filter','NumberTitle','off');
subplot(2,1,1)
% plot(time,force)
hold on
plot(time,force_f)
plot(time,force_filt)
```

```matlab
legend('Filtered Force Data','High Pass Filtered Data')
xlim([start_time stop_time])
% ylim([-3 -2])
grid on
subplot(2,1,2)
plot(time,disp)
hold on
plot(time,disp_f)
legend('Input Displacement Data','Filtered Displacement Data')

time_window = time(time>start_time);

start_value = length(force_filt)-length(time_window)+1;

time_window = time(time<stop_time);
stop_value = length(time_window);

force_section = force_filt(start_value:stop_value);
disp_section = disp_f(start_value:stop_value);
time_section = time(start_value:stop_value);

%% Data analysis section
mdl = fitlm(disp_section,force_section);

%find frequency of oscillation using displacement for test
[pks,pk_indices] = findpeaks(disp_section,1:length(time_sec-
tion),'MinPeakProminence',.005);
td = time_section(pk_indices);
%check = 1./diff(t(1:50)); %check to make sure values are appropriate
freq = 1./mean(diff(td));
total_oscillations = length(pk_indices);
mean_peak_disp = mean(pks);
mean_disp = mean(disp_section);

%find force information for test
[pks,pk_indices] = findpeaks(force_section,1:length(time_sec-
tion),'MinPeakProminence',.05);
tf = time_section(pk_indices);
mean_peak_force = mean(pks);
mean_force = mean(force_section);
equiv_stiff = (mean_peak_force - mean_force)/(mean_peak_disp -
mean_disp);

result = [freq mean_peak_force mean_force mean_peak_disp mean_disp
equiv_stiff]

%create figure to plot force v time and displacement v time with sec-
tioned approach
figure('Name','Axial Force v. Axial Displacement','NumberTitle','off');
subplot(2,1,1)
plot(time_section,force_section,'MarkerIndices',1:length(time_section))
title('Force v. Time')
xlabel('Time [sec]')
ylabel('Axial force [kN]')
grid on
subplot(2,1,2)
```

```matlab
plot(time_section,disp_section,'MarkerIndices',1:length(time_section))
title('Displacement v. Time')
xlabel('Time [sec]')
ylabel('Displacement [mm]')
grid on

%% Overview plot
% first figure shows force over time using section
figure('Name','Overview Graphs','NumberTitle','off');
subplot(2,2,1)
plot(disp_section,force_section)
title('Force v. Displacement')
xlabel('Displacement [mm]')
ylabel('Axial force [kN]')
grid on
% second figure plots the same information, but in context to entire
% testing window
subplot(2,2,2)
plot(disp_section,force_section)
title('Force v. Displacement')
xlabel('Displacement [mm]')
ylabel('Axial force [kN]')
grid on
xlim([-3 3])
ylim([-10 6])
% third figure plots the force and displacement signals over time
subplot(2,2,3)
yyaxis left
plot(time_section,disp_section)
title('Values v. Time')
ylabel('Displacement [mm]')
xlabel('Time [s]')
grid on
% xlim([10 20])
% ylim([-2.5 2.5])
yyaxis right
plot(time_section,force_section)
ylabel('Force [kN]')
% ylim([-10 10])
% fourth figure shows the linear fit for the test case
subplot(2,2,4)
plot(mdl)
title('Linear Fit')
xlabel('Displacement [mm]')
ylabel('Force [kN]')
grid on

% Information regarding linear model fit to force v. displacement
coefficients = mdl.Coefficients;

coefficients(:,1)
mdl.Rsquared


z
```

```matlab
%% Meyer Turku – Master's thesis workbook
% Date: 28 December 2022 Name: Aaron Korkko
% Case Study #2 performed July 2022 on Broneske Mount M01
% close and clear variables
close all
clear
clc

%Inputs for test number and section of test
test_num = 9;    % Identify which test data is being used
section_num = 2;     % Identify which section of data is under analysis
% 1 = 1 Hz, 2 = 2.5Hz, 3 = 5Hz, 4 = 7.5Hz, 5= 10Hz, 6 = 12.5Hz,
% 7 = 15Hz, 8 = 17.5Hz, 9 = 20Hz
pass_band = 2.49;
all_data = 0; %set to 1 for all data in a test set, not subset
windowSize = 10;

% Matrix of start and stop times for frequencies *manually entered*
section = [18          149.5; 152 219.5; 220.5          275.5;
277.5       304; 304.5 318.5; 321 335.5; 349 361.5; 376 387.5; 395.8
           404;
15          148.5; 150.5          209.5; 210.5          241.5; 242 261.5;
263         281; 284.5 298;
299         311.5; 312.5          323.5; 333.5          343.5; 15   149.5;
151         211; 212    241.5;
242         261.5; 263 282; 284.5 298.5; 299.5          311.5; 313
           323.5;325   334.5;
15          149.5; 152 211; 211.5 242.5; 243 262.5; 264 282.5; 284 299;
300         312; 314.5 324; 335   344.5; 15   148.5; 151 210.5; 211.5
           240.5;
242         262; 263   282; 285   298; 300   312; 313.5 323.5; 334.5
           344.5;
15          150.5; 151.5          211; 212   242; 242.5 262; 263    282.5;
284         298.5;
300         312; 313.5 323.5; 334.5          344; 15     150.5; 151 211;
211.5       241;
242         262; 264   282; 283   298; 299   312; 313.5 323.5; 325 335.5];

% Set variables to only look at desired portion of data
row = (test_num–7)*9+section_num;
start_time = section(row,1);
stop_time = section(row,2);

if all_data==1;
    start_time = 0;
    stop_time = 5000;
end

% File names for tests to call based on test_num above
test_names = ["01_preload_0kn_dc_ampl_002mm_1–20z.txt";
    "02_preload_–2.5kn_dc_ampl_002mm_1–20z.txt";
    "03_preload_–5kn_dc_ampl_002mm_1–20z.txt";
    "04_preload_–7.5kn_dc_ampl_002mm_1–20z.txt";
    "05_preload_–9.5kn_dc_ampl_002mm_1–20z.txt";
    "06_preload_2.5kn_dc_ampl_002mm_1–20z.txt";
    "07_preload_5kn_dc_ampl_002mm_1–20z.txt";
```

```matlab
    "08_preload_-9.5kn_dc_ampl_002mm_1-20z.txt";
    "09_preload_-7.5kn_dc_ampl_002mm_1-20z.txt";
    "10_preload_-5kn_dc_ampl_002mm_1-20z.txt";
    "11_preload_-2.5kn_dc_ampl_002mm_1-20z.txt";
    "12_preload_0kn_dc_ampl_002mm_1-20z.txt";
    "13_preload_7.5kn_dc_ampl_002mm_1-20z.txt"];

% Loading of data from file selection
for i=1:length(test_names)
    if test_num == i
        file_name = test_names(i);
    end
end

% Create variable arrays from MTS output data file
array_data = readmatrix(file_name);
count = array_data(:,2);    % cycle count data
disp = array_data(:,3);     % displacement data
force = array_data(:,1);    % force data
time = array_data(:,4);     % time data

%% Cleanup of data to remove NaNs and smoothing of entries
% find NaNs in time matrix and remove entries
purge_t = find(isnan(time));    % store the indices of NaNs in matrix
for removal
flip_purge_t = flipud(purge_t); % flip matrix so removal is possible by
loop
for i=1:length(purge_t)
    j=flip_purge_t(i);
    time(j)=[];
    force(j)=[];
    disp(j)=[];
    count(j)=[];
end
%find NaNs inside of force matrix and remove entries
purge_f = find(isnan(force));   % store the indices of NaNs in matrix
for removal
flip_purge_f = flipud(purge_f); % flip matrix so removal is possible by
loop
for i=1:length(purge_f)
    j=flip_purge_f(i);
    time(j)=[];
    force(j)=[];
    disp(j)=[];
    count(j)=[];
end

%find NaNs inside of displacement matrix and remove all related data
purge_d = find(isnan(disp));    % store the indices of NaNs in matrix
for removal
flip_purge_d = flipud(purge_d); % flip matrix so removal is possible by
loop
for i=1:length(purge_d)
    j=flip_purge_d(i);
    time(j)=[];
    force(j)=[];
```

```matlab
    disp(j)=[];
    count(j)=[];
end

%smooth data by filtering
%windowSize = 10;    % select how many frames the smoothing should occur
b = (1/windowSize)*ones(1,windowSize);
a = 1;
force_f = filter(b,a,force);    % smooth data for force
disp_f = filter(b,a,disp);       % smooth data for displacement

% high pass filter implementation
fs = 10000;
force_filt = highpass(force_f,pass_band,fs);
force_filt = force_filt+mean(force_f);

%plot filtered v. raw signal
figure('Name','Noise Removal v. High Pass Filter','NumberTitle','off');
subplot(2,1,1)
% plot(time,force)
hold on
plot(time,force_f)
plot(time,force_filt)
legend('Filtered Force Data','High Pass Filtered Data')
xlim([start_time stop_time])
% ylim([-3 -2])
grid on
subplot(2,1,2)
plot(time,disp)
hold on
plot(time,disp_f)
legend('Input Displacement Data','Filtered Displacement Data')
%% Windowing from initial section inputs
% create temporary time window for finding the indices of interest with-
out removal of data
time_window = time(time>start_time);    % time data is removed before
desired start time
start_value = length(force_filt)-length(time_window)+1;    %start value
is stored
time_window = time(time<stop_time);    % time data is removed after de-
sired stop time
stop_value = length(time_window);       % stop value is stored

% remove data from force, displacement, and time matrices
force_section = force_filt(start_value:stop_value);    % data between
start and stop time for force selected
disp_section = disp_f(start_value:stop_value);       % data between start
and stop time for displacement selected
time_section = time(start_value:stop_value);          % data between start
and stop time for time data selected

%% Analysis of data with linear regression fit, calculation of frequency
and amplitudes

% fit linear regression model to the force (y) with respect to displace-
ment (x)
```

```matlab
mdl = fitlm(disp_section,force_section);

% find frequency of oscillation using displacement peaks for specified
section of test
[pks,pk_indices] = findpeaks(disp_section,1:length(time_sec-
tion),'MinPeakProminence',.005);
td = time_section(pk_indices);
freq = 1./mean(diff(td));
total_oscillations = length(pk_indices);

% calculate mean peak displacement value and mean displacement value for
section of interest
mean_peak_disp = mean(pks);
mean_disp = mean(disp_section);
max_disp = max(disp_section);
min_disp = min(disp_section);

% calculate mean peak force value and mean force value for section of
interest
[pks,pk_indices] = findpeaks(force_section,1:length(time_sec-
tion),'MinPeakProminence',.05);
tf = time_section(pk_indices);
mean_peak_force = mean(pks);
mean_force = mean(force_section);
max_force = max(force_section);
min_force = min(force_section);

% create figure to display force v time and displacement v time with
correct section and test numbers

figure('Name','Axial Force v. Axial Displacement','NumberTitle','off');
% plot for force v. time
subplot(2,1,1)
plot(time_section,force_section,'MarkerIndices',1:length(time_section))
title('Force v. Time')
xlabel('Time [sec]')
ylabel('Axial force [kN]')
grid on

% plot for displacement v. time
subplot(2,1,2)
plot(time_section,disp_section,'MarkerIndices',1:length(time_section))
title('Displacement v. Time')
xlabel('Time [sec]')
ylabel('Displacement [mm]')
grid on

plot(time_section,disp_section,'MarkerIndices',1:length(time_section))
title('Displacement v. Time')
xlabel('Time [sec]')
ylabel('Displacement [mm]')
grid on

equiv_stiff = (max_force - min_force)/(max_disp - min_disp);
%summary matrix to import to excel
```

```matlab
summary = [freq, max_force, min_force, max_disp, min_disp, equiv_stiff,
mdl.Coefficients.Estimate']

%% Overview plot
% first figure shows force over time using section
figure('Name','Overview Graphs','NumberTitle','off');
subplot(2,2,1)
plot(disp_section,force_section)
title('Force v. Displacement')
xlabel('Displacement [mm]')
ylabel('Axial force [kN]')
grid on
% second figure plots the same information, but in context to entire
% testing window
subplot(2,2,2)
plot(disp_section,force_section)
title('Force v. Displacement')
xlabel('Displacement [mm]')
ylabel('Axial force [kN]')
grid on
xlim([-3 3])
ylim([-10 6])
% third figure plots the force and displacement signals over time
subplot(2,2,3)
yyaxis left
plot(time_section,disp_section)
title('Values v. Time')
ylabel('Displacement [mm]')
xlabel('Time [s]')
grid on
% xlim([10 20])
% ylim([-2.5 2.5])
yyaxis right
plot(time_section,force_section)
ylabel('Force [kN]')
ylim([-10 10])
% fourth figure shows the linear fit for the test case
subplot(2,2,4)
plot(mdl)
title('Linear Fit')
xlabel('Displacement [mm]')
ylabel('Force [kN]')
grid on
```

```matlab
%% Meyer Turku – Master's thesis workbook
% Date: 28 December 2022 Name: Aaron Körkkö
% Case Study #2 performed July 2022 on Broneske Mount L01
% close and clear variables
close all
clear
clc

%Inputs for test number and section of test
test_num = 3;    % Identify which test data is being used
section_num = 7;     % Identify which section of data is under analysis
% [1,2,3,4,5,6,7,8,9] =
[1Hz,2.5Hz,5Hz,7.5Hz,10Hz,12.5Hz,15Hz,17.5Hz,20Hz]
pass_band = 0.99;
all_data = 1; %set to 1 for all data in a test set, not subset

% Matrix of start and stop times for frequencies *manually entered*
section = [2.5         170; 171   236; 238   269; 270   290; 291   305.5;
307        318; 319   329.5; 330.5        339; 340.5 376; 6.5   40.5;
55.5       76;
77.5       100.5; 107 120; 124   137; 142   149; 151   162.5; 166.5 180;
181        197; 90    210; 218.5 277; 286   308; 309 341; 346.5 377.5;
385.5 405;
408        430; 434   445.5; 450 470; 167   280; 281   341; 342   371;
377        398; 399   414.5; 419.5        434; 439   457; 462.5 486;
493        518.5;
93         234; 235.5 292.5; 293.5        323; 327.5 350; 355   370;
376.5      390.5;
394.5      407.5; 412 436; 448   460; 147.5 289.5; 290 349.5; 350 380;
386        418; 434   448.5; 457 470; 476.5 493; 508   520; 525.5 550.5;
148        285; 288   345.5; 348 377.5; 383 432; 439   462; 466.5 481;
486        505.5; 520 554; 561.5 592.5; 124 302; 304   383; 383.5 413;
420        441.5; 447 470; 478   509.5; 515.5        533; 538   552;
558        582;
120.5      273.5; 278.5        337.5; 347.5        381.5; 387 410.5;
429        449;
451        474; 481.5 506.5; 513.5        534; 548.5 573];

% Set variables to only look at desired portion of data
row = (test_num-1)*9+section_num;
start_time = section(row,1);
stop_time = section(row,2);

if all_data==1;
    start_time = 100;
    stop_time = 450;
end

% File names for tests to call based on test_num above
test_names = ["01_preload_0kn_dc_ampl_002mm_1-20z";
    "02_preload_0kn_dc_ampl_002mm_actual_5-20z";
    "03_preload_-7.5kn_dc_ampl_002mm_1-20z.txt";
    "04_preload_7.5kn_dc_ampl_002mm_1-20z.txt";
    "05_preload_15kn_dc_ampl_002mm_1-20z.txt";
    "06_preload_-15kn_dc_ampl_002mm_1-20z.txt";
    "07_preload_-22.5kn_dc_ampl_002mm_1-20z.txt";
```

```matlab
    "08_preload_7.5kn_dc_ampl_004mm_1-20z.txt";
    "09_preload_-7.5kn_dc_ampl_004mm_1-20z.txt"];

% Loading of data from file selection
for i=1:length(test_names)
    if test_num == i
        file_name = test_names(i);
    end
end

% Create variable arrays from MTS output data file
array_data = readmatrix(file_name);
count = array_data(:,1);    % cycle count data
disp = array_data(:,2);     % displacement data
force = array_data(:,3);    % force data
time = array_data(:,4);     % time data

%% Cleanup of data to remove NaNs and smoothing of entries
% find NaNs in time matrix and remove entries
purge_t = find(isnan(time));    % store the indices of NaNs in matrix
for removal
flip_purge_t = flipud(purge_t); % flip matrix so removal is possible by
loop
for i=1:length(purge_t)
    j=flip_purge_t(i);
    time(j)=[];
    force(j)=[];
    disp(j)=[];
    count(j)=[];
end
%find NaNs inside of force matrix and remove entries
purge_f = find(isnan(force));   % store the indices of NaNs in matrix
for removal
flip_purge_f = flipud(purge_f); % flip matrix so removal is possible by
loop
for i=1:length(purge_f)
    j=flip_purge_f(i);
    time(j)=[];
    force(j)=[];
    disp(j)=[];
    count(j)=[];
end

%find NaNs inside of displacement matrix and remove all related data
purge_d = find(isnan(disp));    % store the indices of NaNs in matrix
for removal
flip_purge_d = flipud(purge_d); % flip matrix so removal is possible by
loop
for i=1:length(purge_d)
    j=flip_purge_d(i);
    time(j)=[];
    force(j)=[];
    disp(j)=[];
    count(j)=[];
end
```

```matlab
%smooth data by filtering
windowSize = 10;    % select how many frames the smoothing should occur
b = (1/windowSize)*ones(1,windowSize);
a = 1;
force_f = filter(b,a,force);    % smooth data for force
disp_f = filter(b,a,disp);       % smooth data for displacement

% high pass filter implementation
fs = 1048;
force_filt = highpass(force_f,pass_band,fs);
force_filt = force_filt+mean(force_f);

%plot filtered v. raw signal
figure('Name','Noise Removal v. High Pass Filter','NumberTitle','off');
subplot(2,1,1)
% plot(time,force)
hold on
plot(time,force_f)
plot(time,force_filt)
legend('Filtered Force Data','High Pass Filtered Data')
xlim([start_time stop_time])
xlabel('Time [sec]')
ylabel('Force [kN]')
% ylim([-3 -2])
grid on
subplot(2,1,2)
plot(time,disp)
hold on
plot(time,disp_f)
legend('Input Displacement Data','Filtered Displacement Data')

%% Windowing from initial section inputs
% create temporary time window for finding the indices of interest with-
out removal of data
time_window = time(time>start_time);    % time data is removed before
desired start time
start_value = length(force_filt)-length(time_window)+1;    %start value
is stored
time_window = time(time<stop_time);    % time data is removed after de-
sired stop time
stop_value = length(time_window);       % stop value is stored

% remove data from force, displacement, and time matrices
force_section = force_filt(start_value:stop_value);    % data between
start and stop time for force selected
disp_section = disp_f(start_value:stop_value);     % data between start
and stop time for displacement selected
time_section = time(start_value:stop_value);       % data between start
and stop time for time data selected

%% Analysis of data with linear regression fit, calculation of frequency
and amplitudes

% fit linear regression model to the force (y) with respect to displace-
ment (x)
mdl = fitlm(disp_section,force_section)
```

```matlab
% find frequency of oscillation using displacement peaks for specified
section of test
[pks,pk_indices] = findpeaks(disp_section,1:length(time_sec-
tion),'MinPeakProminence',.005);
td = time_section(pk_indices);
freq = 1./mean(diff(td));
total_oscillations = length(pk_indices);

% calculate mean peak displacement value and mean displacement value for
section of interest
mean_peak_disp = mean(pks);
max_peak_disp = max(pks);
min_disp = min(disp_section);
mean_disp = mean(disp_section);

% calculate mean peak force value and mean force value for section of
interest
[pks,pk_indices] = findpeaks(force_section,1:length(time_sec-
tion),'MinPeakProminence',.05);
tf = time_section(pk_indices);
mean_peak_force = mean(pks);
max_peak_force = max(pks);
min_force = min(force_section);
mean_force = mean(force_section);

% create figure to display force v time and displacement v time with
correct section and test numbers

figure('Name','Axial Force v. Axial Displacement','NumberTitle','off');
% plot for force v. time
subplot(2,1,1)
plot(time_section,force_section,'MarkerIndices',1:length(time_section))
title('Force v. Time')
xlabel('Time [sec]')
ylabel('Axial force [kN]')
grid on

% plot for displacement v. time
subplot(2,1,2)
plot(time_section,disp_section,'MarkerIndices',1:length(time_section))
title('Displacement v. Time')
xlabel('Time [sec]')
ylabel('Displacement [mm]')
grid on

plot(time_section,disp_section,'MarkerIndices',1:length(time_section))
title('Displacement v. Time')
xlabel('Time [sec]')
ylabel('Displacement [mm]')
grid on

%calculate equivalent stiffness from force difference and displacement
%difference
equiv_stiff = (max_peak_force - min_force)/(max_peak_disp - min_disp);
%summary matrix to import to excel
```

```matlab
summary = [freq, max_peak_force, min_force, max_peak_disp, min_disp, ...
equiv_stiff, mdl.Coefficients.Estimate']

%% Overview plot
% first figure shows force over time using section
figure('Name','Overview Graphs','NumberTitle','off');
subplot(2,2,1)
plot(disp_section,force_section)
title('Force v. Displacement')
xlabel('Displacement [mm]')
ylabel('Axial force [kN]')
grid on
% second figure plots the same information, but in context to entire
% testing window
subplot(2,2,2)
plot(disp_section,force_section)
title('Force v. Displacement')
xlabel('Displacement [mm]')
ylabel('Axial force [kN]')
grid on
xlim([-3 3])
ylim([-25 25])
% third figure plots the force and displacement signals over time
subplot(2,2,3)
yyaxis left
plot(time_section,disp_section)
title('Values v. Time')
ylabel('Displacement [mm]')
xlabel('Time [s]')
grid on
xlim([410 410.5])
% ylim([-2.5 2.5])
yyaxis right
plot(time_section,force_section)
ylabel('Force [kN]')
% ylim([-10 10])
% fourth figure shows the linear fit for the test case
subplot(2,2,4)
plot(mdl)
title('Linear Fit')
xlabel('Displacement [mm]')
ylabel('Force [kN]')
grid on

figure('Name','Overview Graphs','NumberTitle','off');
plot(disp_section,force_section)
title('Force v. Displacement')
xlabel('Displacement [mm]','FontSize',16)
ylabel('Force [kN]','FontSize',16)
% ylim([6.9 7.1])
% xlim([-.02 -.01])
grid on
ax = gca;
ax.FontSize = 12;

figure('Name','Overview Graphs','NumberTitle','off');
```

```matlab
plot(mdl)
title('Linear Fit')
xlabel('Displacement [mm]','FontSize',16)
ylabel('Force [kN]','FontSize',16)
grid on
ax = gca;
ax.FontSize = 12;

figure('Name','Force and Displacement','NumberTitle','off');
yyaxis left
plot(time_section,disp_section)
title('Values v. Time')
ylabel('Displacement [mm]')
xlabel('Time [s]')
grid on
xlim([410 410.5])
ylim([-0.02 0.03])
yyaxis right
plot(time_section,force_section)
ylabel('Force [kN]')
ylim([-7.7 -6.8])
```